communications biology

Article

https://doi.org/10.1038/s42003-024-06914-y

Increased GHS-R1a expression in the hippocampus impairs memory encoding and contributes to AD-associated memory deficits

Check for updates

Meng Zhang[1,2,3,4,9], Liu Yang[1,3,9], Jiajia Jia[1,3], Fenghua Xu[1,3], Shanshan Gao[1,3], Fubing Han[5], Mingru Deng[6], Jiwei Wang[1,3], Vincent Li[7], Ming Yu[2], Yuxiang Sun[8], Haicheng Yuan[6], Yu Zhou[1,2,3] ✉ & Nan Li[2] ✉

Growth hormone secretagogue receptor 1a (GHS-R1a), also known as the ghrelin receptor, is an important nutrient sensor and metabolic regulator in both humans and rodents. Increased GHS-R1a expression is observed in the hippocampus of both Alzheimer's disease (AD) patients and AD model mice. However, the causal relationship between GHS-R1a elevation in the hippocampus and AD memory deficits remains uncertain. Here, we find that increasing GHS-R1a expression in dCA1 pyramidal neurons impairs hippocampus-dependent memory formation, which is abolished by local administration of the endogenous antagonist LEAP2. GHS-R1a elevation in dCA1 pyramidal neurons suppresses excitability and blocks memory allocation in these neurons. Chemogenetic activation of those high GHS-R1a neurons during training rescues GHS-R1a overexpression-induced memory impairment. Moreover, we demonstrate that increasing GHS-R1a expression in dCA1 pyramidal neurons hampers these neurons' ability to encode spatial memory and reduces engram size in the dCA1 region. Finally, we show that GHS-R1a deletion mitigates spatial memory deficits in APP/PS1 mice with increased GHS-R1a expression in the hippocampus. Our findings reveal a negative, causal relationship between hippocampal GHS-R1a expression and memory encoding, and suggest that blocking the abnormal increase in GHS-R1a activity/expression may be a promising approach to improve memory and treat cognitive decline in AD.

Ghrelin is an orexigenic brain-gut hormone predominantly synthesized in the stomach and is critical for feeding, glucose metabolism, and energy homeostasis[1]. Circulating ghrelin is capable of crossing the blood-brain barrier (BBB) and binds to its receptor, the growth hormone secretagogue receptor 1a (GHS-R1a) in different brain regions including the hypothalamus and the hippocampus[2]. Studies, especially pharmacological studies, have highlighted intriguing yet conflicting roles for the ghrelin/GHS-R1a system in regulating multiple neuronal functions besides nutrient sensing and metabolic control, including learning and memory, reward and motivation, stress responses, anxiety, depression, among others[3,4]. Noticeably, increased GHS-R1a expression has been found in the hippocampus of patients with Alzheimer's disease (AD) and mice that mimic AD amyloidopathy[5]. However, the causal relationship between GHS-R1a elevation in the hippocampus and AD memory deficits remains uncertain. So far, few studies have reported a direct impact of increasing GHS-R1a expression on neuronal function and memory performance under physiological or pathological conditions.

[1]Department of Physiology and Pathophysiology, School of Basic Medical Sciences, Qingdao University, Qingdao, Shandong, 266071, China. [2]Department of Health and Life Sciences, University of Health and Rehabilitation Sciences, Qingdao, Shandong, 266000, China. [3]Institute of Brain Sciences and Related Disorders, Qingdao University, Qingdao, Shandong, 266071, China. [4]College of Agriculture and Bioengineering, Heze University, Heze, Shandong, 274000, China. [5]Department of Neurosurgery, The Affiliated Hospital of Qingdao University, Qingdao, Shandong, 266003, China. [6]Department of Neurology, Affiliated Qingdao Central Hospital, University of Health and Rehabilitation Sciences (Qingdao Central Medical Group), Qingdao, Shandong, 266042, China. [7]Beverly Hills High School, Beverly Hills, CA, 90212, USA. [8]Department of Nutrition, Texas A&M University, College Station, TX, 77843, USA. [9]These authors contributed equally: Meng Zhang, Liu Yang. ✉e-mail: yuzhou@qdu.edu.cn; linan@uor.edu.cn

It is important to note that while ghrelin action requires binding to GHS-R1a, GHS-R1a itself displays high constitutive activity in the absence of ligands such as ghrelin[6,7]. The ligand-independent activity of GHS-R1a has also been shown to be functionally relevant in controlling food intake, regulating growth hormone release and body length, and affecting memory processes[8,9]. Furthermore, the fact that GHS-R1a can form heterodimers with various other receptors, including dopamine receptors, serotonin receptors and oxytocin receptors, to affect downstream signaling and receptor trafficking[10–12], weights complexity and diversity of GHS-R1a function. The liver-expressed antimicrobial peptide 2 (LEAP2) was recently identified to act as an endogenous antagonist/inverse agonist of GHS-R1a to control both its ligand-dependent and ligand-independent activity in response to the feeding status[13]. Thus, the neuronal function of GHS-R1a may not be solely dependent on the binding of ghrelin, and changes in overall GHS-R1a expression/activity might have distinct biological outcomes from that of ghrelin-dependent activation, under both physiological and pathological conditions like AD.

In this study, we sought to determine how a direct increase of GHS-R1a expression in dorsal hippocampus modulates hippocampus-dependent memory, and how GHS-R1a deletion affects memory deficit in APP/PS1 mice showing elevated GHS-R1a expression in the hippocampus. Our findings reveal a negative, causal relationship between hippocampal GHS-R1a expression and memory encoding, and suggest that blocking the abnormal increase in GHS-R1a expression/activity in the hippocampus may be a promising approach to treat disease-associated cognitive decline, such as in AD.

Result

Increasing GHS-R1a expression in dCA1 pyramidal neurons impairs memory

We delivered *aav-hSyn-DIO-Ghsr1a-2A-eGFP* virus to hippocampal dCA1 of *Camk2a-Cre* mice (Fig. 1a, b–d), as well as *aav-Camk2a-Ghsr1a-2A-eGFP* virus to dCA1 of wild-type (WT) C57BL/6 mice (Fig. 1a, e–g) in order to increase GHS-R1a expression selectively in pyramidal neurons of dorsal hippocampus, mainly the dCA1 region. Predominant GFP fluorescence in dCA1 pyramidal neurons indicated successful viral transfection and GHS-R1a expression (Fig. 1b, e). First, we compared the performance of GHS-R1a-overexpressing mice and control mice in an object-location recognition (OLR) task. Our results demonstrated that both GHS-R1a-overexpressing *Camk2a-Cre* mice (Fig. 1c) and GHS-R1a-overexpressing WT mice (Fig. 1f) spent significantly less time than controls receiving *aav-DIO-eGFP* or *aav-eGFP* viral transfection, exploring the new-location object, indicating that elevating GHS-R1a expression impairs object-location memory (Fig. 1c Left; Unpaired *t* test, *aav-DIO-eGFP* vs. *aav-DIO-Ghsr1a-eGFP*, $t = 3.64$, $P < 0.01$. Figure 1f Left; Unpaired *t* test, *aav-eGFP* vs. *aav-Ghsr1a-eGFP*, $t = 3.09$, $P < 0.01$). In addition, our results showed that control mice spent significantly more percentage of time than random (50%) exploring new-location object (Fig. 1c, f Left; One sample *t* test, *aav-DIO-eGFP*: $t = 7.05$, $P < 0.001$; *aav-eGFP*: $t = 3.82$, $P < 0.01$), while the GHS-R1a-overexpressing mice did not (Fig. 1c, f Left; One sample *t* test, *aav-DIO-Ghsr1a-eGFP*: $t = 0.69$, $P > 0.05$; *aav-Ghsr1a-eGFP*: $t = 0.51$, $P > 0.05$), supporting impaired object-location memory caused by GHS-R1a elevation in dCA1 pyramidal neurons. Morris water maze (MWM) probe tests also revealed that GHS-R1a upregulation impaired spatial memory

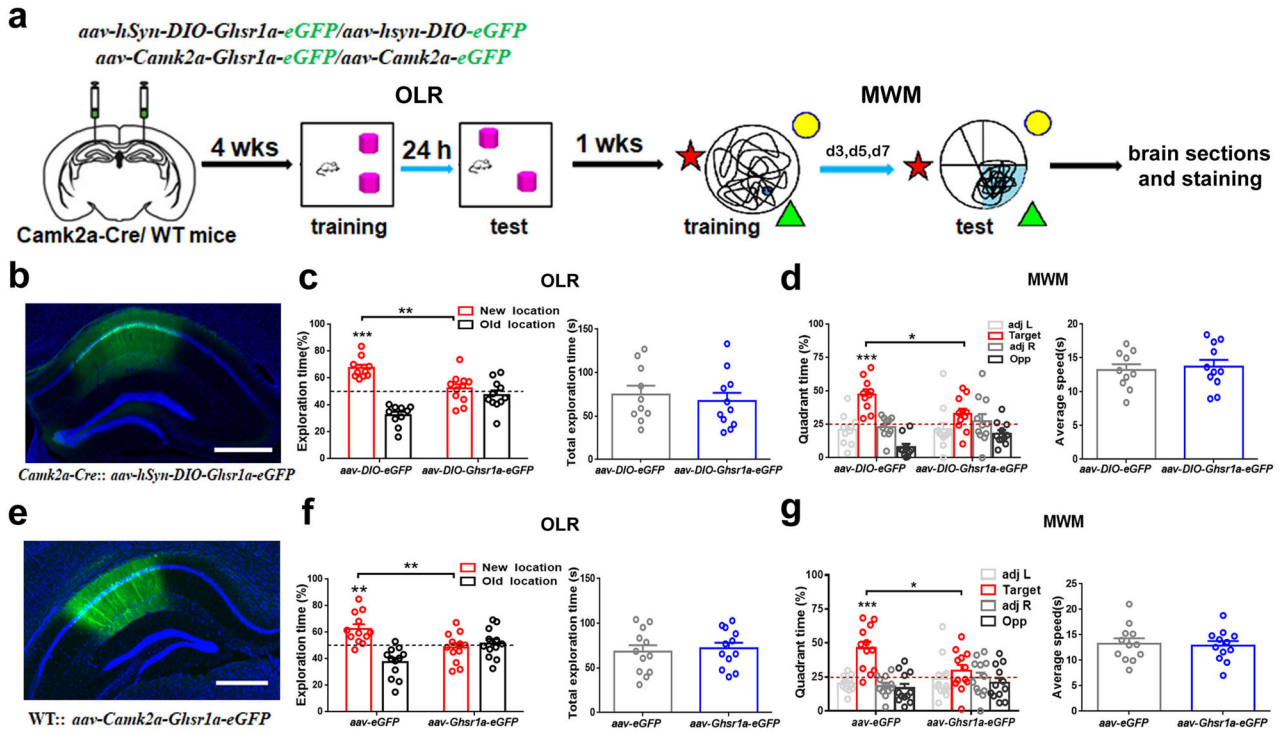

Fig. 1 | GHS-R1a overexpression in dCA1 pyramidal neurons impairs spatial and open-location memory. a A flow chat illustrating experimental design. **b** A representative image taken 4 weeks after *aav-hSyn-DIO-Ghsr1a-2A-eGFP* virus delivery in dCA1 of a *Camk2a-Cre* mouse. GFP (green), DAPI (blue). Scale bar, 500 μm. **c** The OLR test in *Camk2a-Cre* mice. ***Left***, exploration time (%) in the new-location object. ***Right***, the total objects exploration time. **d** The Morris water maze probe test in *Camk2a-Cre* mice. ***Left***, searching time (%) in target quadrant at the 7th day probe test. ***Right***, swimming speed during the probe test. $n = 11–12$ mice per group. **e** A representative image showing GFP fluorescence in dCA1 of a C57BL/6 mouse receiving *aav-Camk2a-Ghsr1a-2A-eGFP* virus injection 4 weeks ago. GFP (green), DAPI (blue). Scale bar, 500 μm. **f** The OLR memory assays in C57BL/6 mice. n = 12 mice per group. **g** Spatial memory assays in C57BL/6 mice. All data is shown as means ± SEM. $^{***}P < 0.001$, $^{**}P < 0.01$ or $^{*}P < 0.05$ means significant difference.

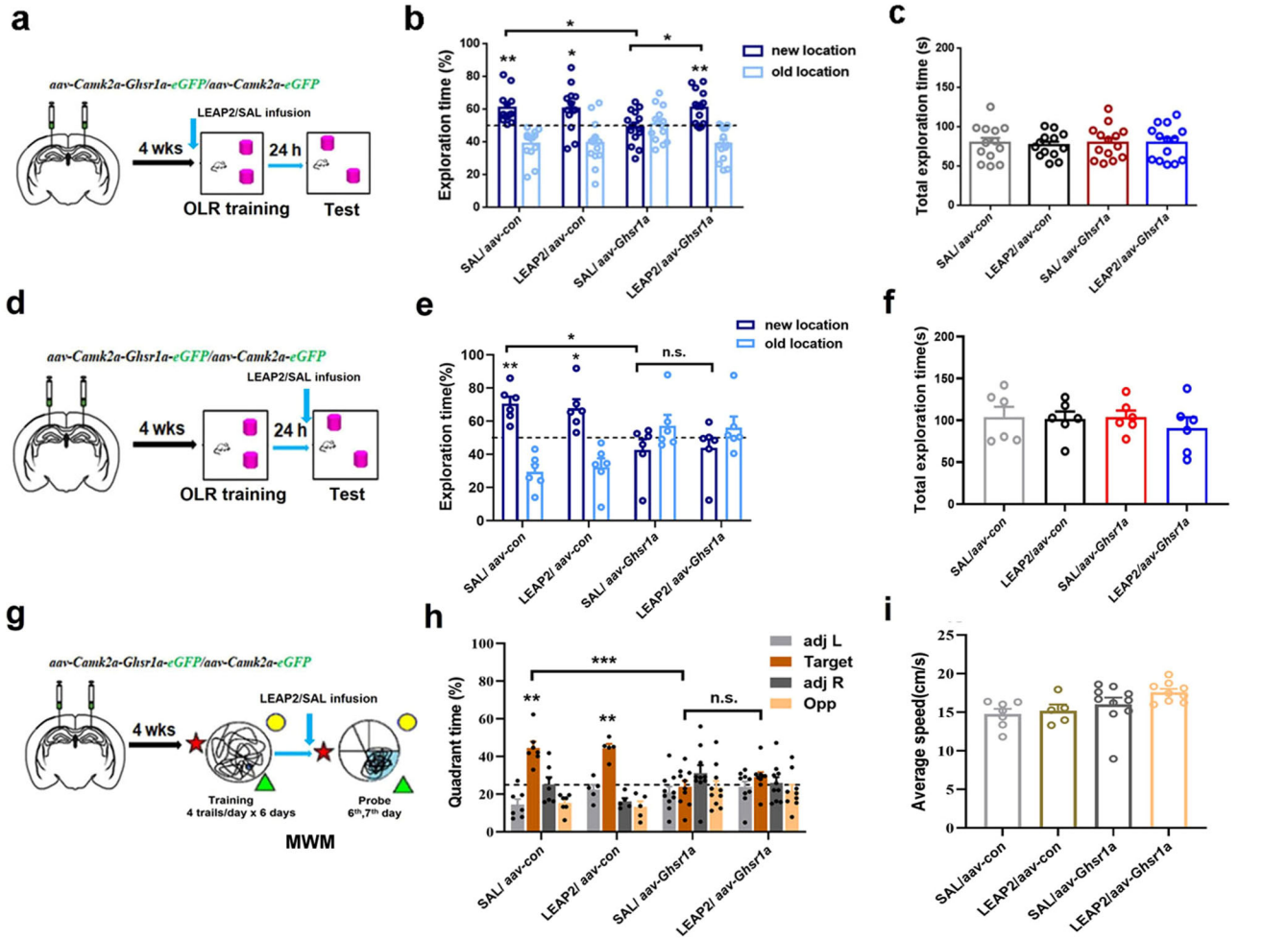

Fig. 2 | LEAP2 administration during training blocks the suppressive effect of increased GHS-R1a expression on memory. a Diagram illustrating experimental pipeline. LEAP2 or SAL vehicle was delivered in dCA1 at 20 min before OLR training in mice previously transduced with *aav-Camk2a-Ghsr1a* virus or control *aav-Camk2a-eGFP* virus. **b** The OLR memory assays. **c** Total object exploration time during memory test. SAL/*aavcon* ($n = 13$), LEAP2/*aav-con* ($n = 13$), SAL/*aav-Ghsr1a* ($n = 14$), LEAP2/*aav-Ghsr1a* ($n = 14$). **d** Diagram illustrating experimental pipeline. LEAP2 or SAL were administrated 20 min before the OLR memory test. **e** The OLR memory assays. **f** Total objects exploration time during the OLR memory test. $n = 6$ mice per group **g** Diagram illustrating experimental pipeline. LEAP2 or SAL vehicle were administrated 20 min before the MWM probe test. **h** Searching time (%) in target quadrant at the 7th day probe test. **i** Swimming speed comparison during the probe test. SAL/*aavcon* ($n = 7$), LEAP2/*aav-con* ($n = 5$), SAL/*aav-Ghsr1a* ($n = 10$), LEAP2/*aav-Ghsr1a* ($n = 9$). All data is shown as means ± SEM. $^{**}P < 0.01$ or $^{*}P < 0.05$ means significant difference.

(Fig. 1d Left; Unpaired *t* test, *aav-DIO-Ghsr1a-eGFP* vs. *aav-DIO-eGFP*, $t = 2.69$, $P < 0.05$. Figure 1g Left; Unpaired *t* test, *aav-Ghsr1a-eGFP* vs. *aav-eGFP*, $t = 2.14$, $P < 0.05$). Clearly, control mice spent significantly more percentage of time than random (25%) navigating the target quadrant during the probe test (Fig. 1d, g Left; One sample *t* test, *aav-DIO-eGFP*: $t = 5.82$, $P < 0.001$; *aav-eGFP*: $t = 4.51$, $P < 0.001$), while the GHS-R1a-overexpressing mice did not (Fig. 1d, g Left; One sample *t* test, *aav-DIO-Ghsr1a-eGFP*: $t = 2.11$, $P > 0.05$; *aav-Ghsr1a-eGFP*: $t = 1.80$, $P > 0.05$). There was no difference between GHS-R1a-overexpressing mice and controls as for the total objects exploration time during the OLR test (Fig. 1c, f Right; Unpaired *t* test, *aav-DIO-eGFP* vs. *aav-DIO-Ghsr1a-eGFP*: $t = 0.55$, $P > 0.05$; *aav-eGFP* vs. *aav-Ghsr1a-eGFP*: $t = 0.40$, $P > 0.05$) and the swimming speed during the MWM probe test (Fig. 1d, g Right; Unpaired *t* test, *aav-DIO-eGFP* vs. *aav-DIO-Ghsr1a-eGFP*: $t = 0.40$, $P > 0.05$; *aav-eGFP* vs. *aav-Ghsr1a-eGFP*: $t = 0.28$, $P > 0.05$). In addition, we did not find significant difference between GHS-R1a-overexpressing mice and controls regarding to objects exploration time and latency to platform during training sessions (Supplementary Fig. 1a-d). We confirmed virus-mediated GHS-R1a overexpression in dCA1 pyramidal neurons through fluorescent in situ hybridization (FISH) images (Supplementary Fig. 1e, f). Taken together, our findings indicate that increasing GHS-R1a expression in dCA1 pyramidal neurons impairs hippocampus-dependent memory.

LEAP2 administration during learning rescues memory impairment caused by GHS-R1a overexpression in dCA1 pyramidal neurons

LEAP2 was recently reported to be an endogenous antagonist of GHS-R1a, which also exhibited inverse agonist activity[14]. To determine whether memory impairment caused by elevated GHS-R1a expression in dCA1 pyramidal neurons could be blocked by antagonizing GHS-R1a activity, we micro-infused LEAP2 (10 ng, 0.5ul/side) or saline vehicle (SAL) in dorsal hippocampus of GHS-R1a-overexpressing mice (LEAP2/*aav-Ghsr1a* or SAL/*aav-Ghsr1a*) and control mice (LEAP2/*aav-con* or SAL/*aav-con*) respectively, at 20 min before the start of OLR training. Specifically, the mice were previously transfected with *aav-Camk2a-Ghsr1a-2A-eGFP* virus or control *aav-Camk2a-eGFP* virus in the dCA1 region (Fig. 2a). Our results consistently demonstrated that elevated GHS-R1a expression in dCA1 pyramidal neurons led to memory deficit in OLR (Fig. 2b; Two-way ANOVA, viral infection $F_{(1,\ 50)} = 3.54$, $P = 0.07$; drug treatment $F_{(1,\ 50)} = 3.70$, $P = 0.06$; interaction $F_{(1,\ 50)} = 4.11$, $P < 0.05$; Tukey's multiple comparisons test, SAL/*aav-Ghsr1a* vs. SAL/

aav-con, $P < 0.05$). Importantly, we found that acute LEAP2 administration during the OLR training rescued memory impairment caused by GHS-R1a overexpression (Fig. 2b; LEAP2/*aav-Ghsr1a* vs. SAL/*aav-Ghsr1a*, $P < 0.05$). The dosage of LEAP2 was chosen based on both pilot studies and previous report[14]. There was no difference among the four groups of mice as for the total objects exploration time during the OLR test (Fig. 2c; Two-way ANOVA, viral infection $F_{(1,\ 50)} = 0.12$, $P > 0.05$; drug treatment $F_{(1,\ 50)} = 0.08$, $P > 0.05$; interaction $F_{(1,\ 50)} = 0.06$, $P > 0.05$).

Next, we investigate whether memory impairment caused by elevating GHS-R1a expression could be improved by antagonizing GHS-R1a activity during memory retrieval.

To this end, we micro-infused LEAP2 or SAL in the dorsal hippocampus of GHS-R1a-overexpressing mice and controls at 20 min before the test (Fig. 2d, g). Our results demonstrated that LEAP2 treatment was not able to rescue GHS-R1a overexpression-induced memory impairment (Fig. 2e; Two-way ANOVA, viral infection $F_{(1,\ 20)} = 20.13$, $P < 0.001$; drug treatment $F_{(1,\ 20)} = 0.02$, $P > 0.05$; interaction $F_{(1,\ 20)} = 0.12$, $P > 0.05$; Tukey's multiple comparisons test, LEAP2/*aav-Ghsr1a* vs. SAL/*aav-Ghsr1a*, $P > 0.05$). There is no difference in total objects exploration time among four groups of mice (Fig. 2f; Two-way ANOVA, $P > 0.05$). Consistently, we also found that acute LEAP2 treatment during the spatial memory recall failed to rescue GHS-R1a overexpression-induced spatial memory impairment (Fig. 2h; Two-way ANOVA, viral infection $F_{(1,\ 27)} = 32.36$, $P < 0.0001$; drug treatment $F_{(1,\ 27)} = 0.60$, $P > 0.05$; interaction $F_{(1,\ 27)} = 0.68$, $P > 0.05$; Tukey's multiple comparisons test, LEAP2/*aav-Ghsr1a* vs. SAL/*aav-Ghsr1a*, $P > 0.05$). Clearly, control mice spent significantly more percentage of time than random (25%) navigating the target quadrant during the probe test (Fig. 2h; One sample *t* test, SAL/ *aav-con*, $t = 5.733$, $P < 0.01$; LEAP2/ *aav-con*, $t = 8.219$, $P < 0.01$); while GHS-R1a-overexpressing mice did not regardless of LEAP2 treatment or not (Fig. 2h; One sample *t* test, SAL/ *aav-Ghsr1a*, $t = 0.1468$, $P > 0.05$; LEAP2/ *aav-Ghsr1a*, $t = 2.026$, $P > 0.05$). Four groups of mice exhibited similar swimming speed during the probe test (Fig. 2i), and similar latencies to the platform across 6 training days (Supplementary Fig. 2). Altogether, our findings demonstrate that antagonizing GHS-R1a activity during training, but not during the test, improves memory impairment caused by virus-mediated GHS-R1a overexpression in dorsal CA1 hippocampus. Previously, we have reported that local infusion of ghrelin blocks memory acquisition, while it has no significant effect on consolidation or retrieval processes[15,16]. Therefore, we propose that increasing GHS-R1a expression in dCA1 pyramidal neurons may disrupts memory encoding and initial consolidation, leading to hippocampus-dependent memory formation deficit.

Increasing GHS-R1a expression suppresses excitability of dCA1 pyramidal neurons

To explore the physiological mechanism mediating the inhibitory effect of GHS-R1a on memory, we tested whether increasing GHS-R1a expression in dCA1 pyramidal neurons affected neuronal excitability, synaptic transmission, and plasticity. Acute dorsal hippocampal slices were prepared four weeks after delivery of *aav-Camk2a-Ghsr1a-2A-eGFP* virus or control *aav-Camk2a-eGFP* virus. We found that an increase in GHS-R1a expression caused a significant decrease in the excitability of dCA1 pyramidal neurons. Specifically, the number of action potentials (APs) triggered by depolarizing current injections (≥150 pA, 600 ms in duration) was significantly less in GHS-R1a-overexpressing neurons than in controls (Fig. 3a; Two-way repeated measure ANOVA, viral infection $F_{(1,\ 32)} = 20.17$, $P < 0.0001$; stimulus intensity $F_{(12,\ 384)} = 76.02$, $P < 0.0001$; interaction $F_{(12,\ 384)} = 8.71$, $P < 0.0001$. Sidak's multiple comparisons test, *aav-eGFP* vs. *aav-Ghsr1a-eGFP*, $P < 0.01$ to $P < 0.0001$). Further analyses showed that a strong depolarizing current (700pA, 50 ms in duration) triggered high GHS-R1a neurons to fire with a larger inter-spike interval (ISI), a bigger AP half-width and a larger fast afterhyperpolarization potential (fAHP) than control neurons, indicating reduced excitability (Fig. 3b–e; Unpaired *t* test, *aav-Ghsr1a-eGFP* vs. *aav-eGFP*, ISI: $t = 2.55$, $P < 0.05$; AP half-width: $t = 3.38$, $P < 0.01$; fAHP: $t = 2.27$, $P < 0.05$). Two groups of neurons exhibited similar input resistances, resting membrane potentials (RMPs), AP thresholds, and rheobase (Fig. 3f–i). Moreover, high GHS-R1a-induced inhibition of neuronal firing was simulated by acute application of acylated ghrelin, the endogenous ligand for GHS-R1a, to dCA1 pyramidal neurons (Fig. 3j; Two-way repeated measure ANOVA, drug treatment $F_{(1,\ 34)} = 13.17$, $P < 0.001$; stimulus intensity $F_{(15,\ 510)} = 177.7$, $P < 0.0001$; interaction $F_{(15,\ 510)} = 3.70$, $P < 0.0001$. Sidak's multiple comparisons test, ACSF vs. ghrelin, $P < 0.05$ to $P < 0.0001$). We also confirmed ex vivo that chemogenetic activation of dCA1 pyramidal neurons by bath application of CNO (20 μM) could abolish the suppressive effect of high GHS-R1a expression on neuronal excitability (Fig. 3k–n). A hM3Dq-DREADD virus with concurrent GHS-R1a expression (*aav-Camk2a-hM3D(Gq)-2A-Ghsr1a-sfGFP*) was pre-delivered in mice dCA1 area to selectively express both hM3Dq and GHS-R1a in a population of pyramidal neurons (Fig. 3k). Our results demonstrated that CNO administration increased firing of high GHS-R1a neurons (Fig. 3l; Two-way repeated measure ANOVA, drug treatments $F_{(1,\ 156)} = 115.7$, $P < 0.0001$; stimulus intensity $F_{(12,\ 156)} = 38.65$, $P < 0.0001$; interaction $F_{(12,\ 156)} = 2.36$, $P < 0.001$. Sidak's multiple comparisons test, *aav-hM3D(Gq)-Ghsr1a*/CNO vs. *aav-hM3D(Gq)-Ghsr1a*/SAL, $P < 0.05$ to $P < 0.001$). In particular, CNO administration triggered high GHS-R1a neurons to fire with a shorter AP half-with (Fig. 3m; Unpaired *t* test, $t = 2.81$, $P < 0.05$) and a smaller fAHP amplitude (Fig. 3n; Unpaired *t* test, $t = 2.239$, $P < 0.05$). We thus concluded that elevating GHS-R1a expression decreases intrinsic excitability of dCA1 pyramidal neurons.

In addition, we found that elevating GHS-R1a expression did not affect miniature or spontaneous excitatory postsynaptic currents (mEPSCs or sEPSCs) (Supplementary Fig. 3a, b). Ex vivo field EPSPs (fEPSPs) recording in the Schaffer collaterals (SC)-CA1 synapses of *aav-Ghsr1a* virus-transduced dCA1 pyramidal neurons also revealed a normal synaptic input/output relationship, normal paired-pulse ratio (PPR), and normal LTP (Supplementary Fig. 3c–e). These findings indicate that increasing GHS-R1a expression in dCA1 pyramidal neurons had no significant impact on synaptic transmission or plasticity of SC-CA1 synapses. Therefore, we conclude that a decrease in intrinsic excitability of dCA1 pyramidal neurons, rather than synaptic modification, could be a key mechanism mediating high GHS-R1a-induced memory impairment in adult mice.

Chemogenetic activation of dCA1 pyramidal neurons with high GHS-R1a expression rescues memory impairment in those mice

Next, we tested whether memory impairment caused by increased GHS-R1a expression in dCA1 pyramidal neurons could be rescued by chemogenetic activation of those neurons during the learning phase. The *aav-Camk2a-hM3D(Gq)-2A-Ghsr1a-sfGFP* or *aav-Camk2a-hM3D(Gq)-2A-sfGFP* virus, as well as the control virus lacking the hM3Dq construct (*aav-Camk2a-Ghsr1a-eGFP* or *aav-Camk2a-eGFP*) were injected into the dCA1 area to selectively express both hM3Dq and GHS-R1a, either hM3Dq or GHS-R1a, or GFP only in a population of pyramidal neurons. All eight groups of mice were trained in a MWM task (4 trails/day for 6 days) and CNO (1 mg/kg) or saline vehicle (SAL) was applied by intraperitoneal (i.p.) injection 45 min before the start of daily training (Fig. 4a). Ex vivo slice recording confirmed that CNO (20 μM) administration selectively promoted depolarization-evoked firing in pyramidal neurons expressing hM3Dq, not in control neurons lack of hM3Dq (Fig. 4b). MWM probe tests consistently revealed that increasing GHS-R1a expression impaired spatial memory. Both *aav-hM3D(Gq)-Ghsr1a*/SAL and *aav-Ghsr1a*/SAL mice spent random time (25%) searching the target quadrant (Fig. 4c,d; One sample *t* test, *aav-hM3D(Gq)-Ghsr1a*/SAL, $t = 1.563$, $P > 0.05$; *aav-Ghsr1a*/SAL, $t = 2.038$, $P > 0.05$), which is significantly less than control *aav-hM3D(Gq)*/SAL mice (Fig. 4c; Two-way ANOVA, viral infection $F_{(1,\ 24)} = 4.58$, $P < 0.05$; drug treatment $F_{(1,\ 24)} = 6.97$, $P < 0.05$; interaction $F_{(1,\ 24)} = 3.25$, $P = 0.08$. Tukey's multiple comparisons test, *aav-hM3D(Gq)-Ghsr1a*/SAL vs. *aav-hM3D(Gq)*/SAL, $P < 0.05$), and control *aav-eGFP*/SAL mice without GHS-R1a overexpression (Fig. 4d; viral infection $F_{(1,\ 24)} = 17.26$, $P < 0.001$; drug treatment $F_{(1,\ 24)} = 0.004$, $P > 0.05$; interaction, $F_{(1,\ 24)} = 0.07$, $P > 0.05$.

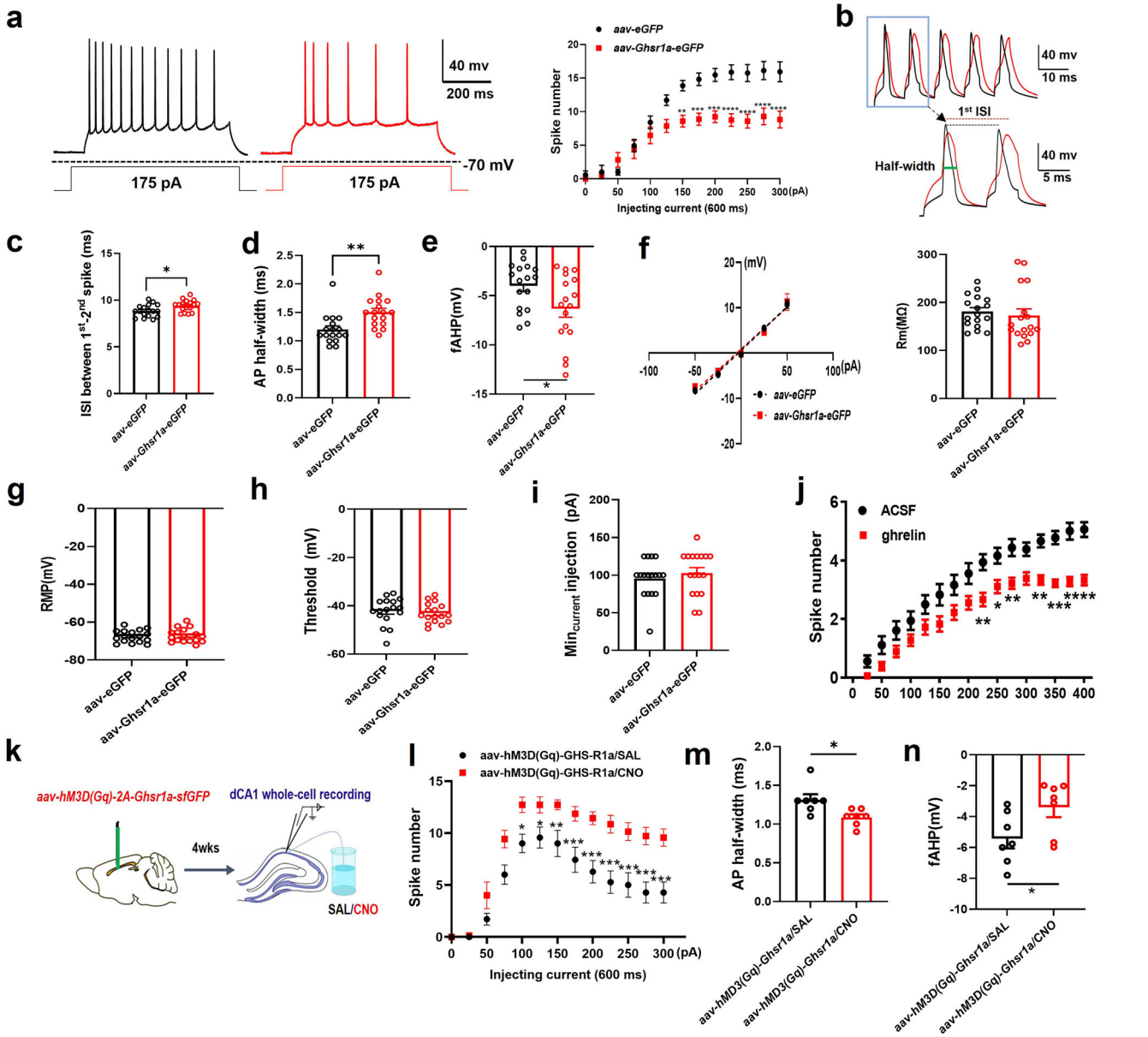

Fig. 3 | Increasing GHS-R1a expression suppresses excitability of dCA1 pyramidal neurons. a Comparison of firings evoked by current injections. Mice were transduced with control *aav-eGFP* virus (black) or *Ghsr1a*-expressing virus (red) in dCA1 4 weeks ahead. ***Left***, representative firing of dCA1 pyramidal neurons in response to a 175 pA current injection. ***Right***, the number of action potentials triggered by a series of depolarizing currents in high GHS-R1a neurons and in control neurons. **b–i** Comparison of firing properties between two groups of neurons under short-duration (50 ms) injecting currents. Firings triggered by a strong depolarizing current (700pA, 50 ms in duration) in sample neurons (**b**), inter-spike interval (**c**), AP half-width (**d**), fAHP (**e**), input resistance (**f**), RMP (**g**), threshold (**h**), and rheobase (**i**). High GHS-R1a neurons, n = 17 from 5 mice; control neurons, $n = 17$ from 5 mice. (**j**) Acute application of ghrelin to dCA1 pyramidal neurons inhibited neuronal firing. $n = 15$ cells from 5 mice per group. (**k**) Diagram illustrating experimental pipeline. The *aav-Camk2a-hM3D(Gq)-2A-Ghsr1a-sfGFP* virus was pre-delivered in mice dCA1 area at 4 weeks before the ex vivo recordings. **l–n** Firing properties of hM3D(Gq)-GHS-R1a neurons evoked by current injection (600 ms) with bath application of SAL or CNO. Firing pattern (**l**), AP half-width (**m**), and fAHP (**n**). $n = 7$ cells from 3 mice per group. All data is shown as means ± SEM., $^{****}P < 0.0001$, $^{***}P < 0.001$, $^{**}P < 0.01$ or $^{*}P < 0.05$ means significant difference.

Tukey's multiple comparisons test, *aav-Ghsr1a*/SAL vs. *aav-eGFP*/SAL, $P < 0.05$). Noticeably, *aav-hM3D(Gq)-Ghsr1a*/CNO mice spent significantly more time than random (25%) navigating the target quadrant (Fig. 4c; One sample *t* test, $t = 6.63$, $P < 0.0001$), indicating normal spatial memory. The higher target quadrant searching time in *aav-hM3D(Gq)-Ghsr1a*/CNO mice than that in *aav-hM3D(Gq)-Ghsr1a*/SAL mice (Fig. 4c; $P < 0.05$) confirm that CNO-mediated activation of the hM3Dq-DREADD during MWM training rescues spatial memory impairment caused by increased GHS-R1a expression in dCA1 pyramidal neurons. Importantly, CNO administration had no effect on spatial memory performance of either *aav-Ghsr1a-eGFP* mice or *aav-eGFP* mice, in comparison to SAL-treated groups (Fig. 4d; *aav-Ghsr1a-eGFP*/CNO vs. *aav-Ghsr1a-eGFP*/SAL, $P > 0.05$; *aav-eGFP*/CNO vs. *aav-eGFP*/SAL, $P > 0.05$), indicating that the rescue effect of CNO on *aav-hM3D(Gq)-Ghsr1a* mice is specific.

Consistently, we found that chemogenetic activation of those dCA1 neurons also rescued OLR memory impairment in high GHS-R1a-expressing mice (Fig. 4e, f). CNO administration during training did not affect total objects exploration time (Fig. 4e), however, it significantly increased exploration time in new-location object in *aav-hM3D(Gq)-Ghsr1a* mice (Fig. 4f; Two-way ANOVA, viral infection $F_{(1,\ 50)} = 4.57$,

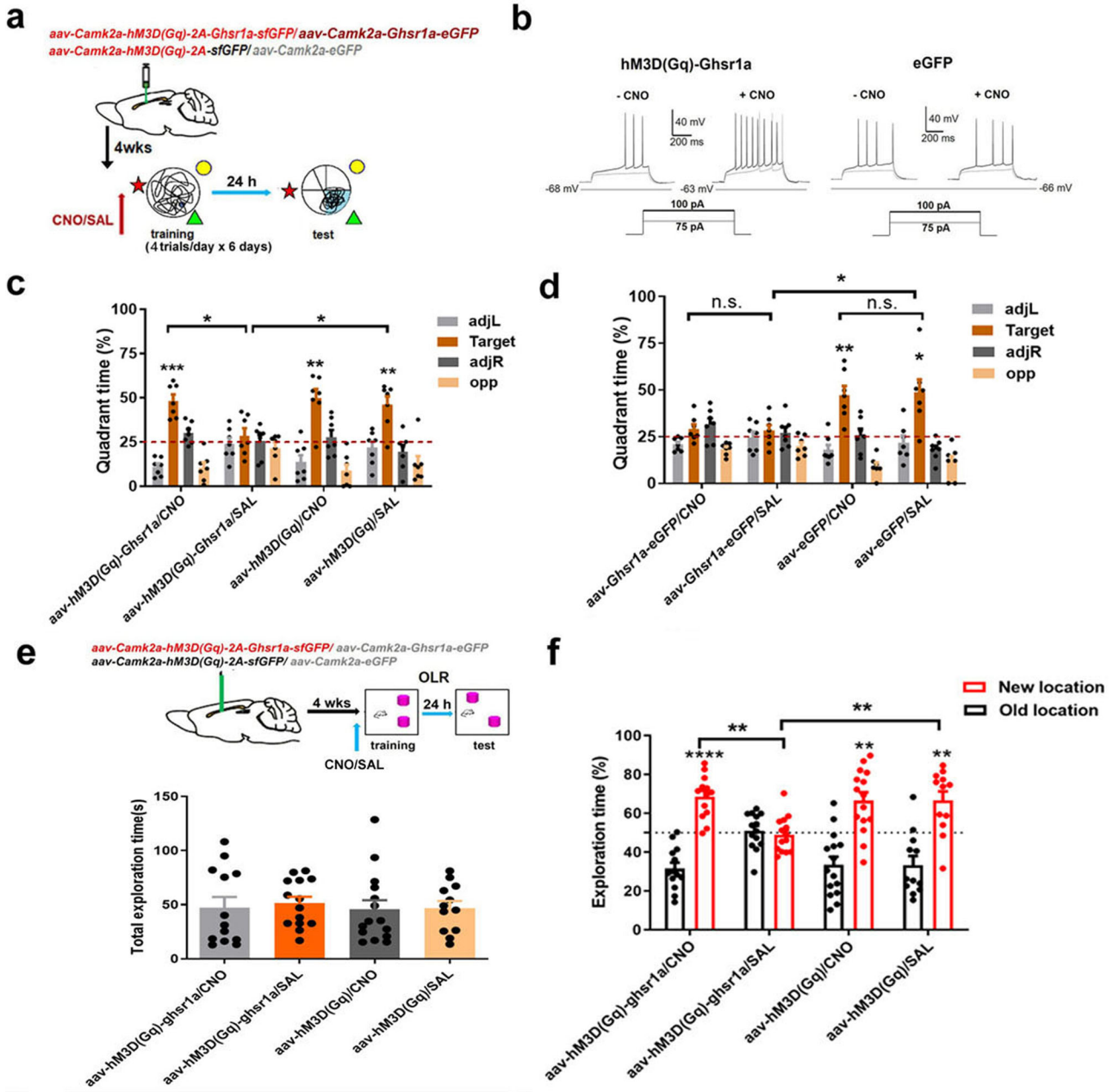

Fig. 4 | Chemogenetic activation of those dCA1 pyramidal neurons with GHS-R1a overexpression rescues memory impairment. (**a**) Diagram illustrating experimental pipeline. CNO (1 mg/kg) or SAL was applied by i.p. injection at 45 min before the start of daily MWM training (4 trails/day) for 6 days. **b** Sample Ex vivo slice recordings. CNO, 20 μM. **c–d** Spatial memory comparison among groups of mice. $n = 7$ mice per group. **e–f** Chemogenetic activation of those GHS-R1a-overexpressed neurons rescues the OLR memory deficit. **e** Total objects exploration time. **f** Exploration time (%) in the new-location object during the test. $n = 12–15$ mice per group. All data is shown as means ± SEM. $^{****}P < 0.0001$, $^{**}P < 0.01$ or $^{*}P < 0.05$ means significant difference, n.s. means no significance.

$P < 0.05$; drug treatment $F_{(1,\ 50)} = 6.93$, $P < 0.05$; interaction, $F_{(1,\ 50)} = 7.01$, $P < 0.05$. Tukey's multiple comparisons test, *aav-hM3D(Gq)-Ghsr1a*/CNO vs. *aav-hM3D(Gq)-Ghsr1a*/SAL, $P < 0.01$). Remarkably, the *aav-hM3D(Gq)-Ghsr1a*/CNO mice spent more time than random (50%) exploring the object in new location (Fig. 4f; One sample *t* test, $t = 6.043$, $P < 0.0001$), while the *aav-hM3D(Gq)-Ghsr1a*/SAL mice did not (Fig. 4f; One sample *t* test, $t = 0.42$, $P > 0.05$). Altogether, our findings demonstrate that increasing excitability of dCA1 pyramidal neurons with high GHS-R1a expression during training improves both the OLR memory and the spatial memory. We thus reach a conclusion that reduced excitability of dCA1 pyramidal neurons contributes to high GHS-R1a-induced memory impairment.

Increasing GHS-R1a expression excludes those dCA1 pyramidal neurons from memory encoding

Previous studies, including our own work, have highlighted the importance of neuronal excitability in determining cellular allocation of engrams in neural circuits[17–19]. To explore the network mechanism underlying GHS-R1a-induced memory impairment, we tested whether increasing GHS-R1a expression in a population of dCA1 pyramidal neurons affects memory allocation in the hippocampus. First, we injected a hM4Di-DREADD virus with or without concurrent GHS-R1a expression (*aav-Camk2a-hM4D(Gi)-2A-Ghsr1a-sfGFP* or *aav-Camk2a-hM4D(Gi)-2A-sfGFP*), as well as control viruses lacking the hM4Di construct (*aav-Camk2a-Ghsr1a-eGFP* or *aav-Camk2a-eGFP*) into the

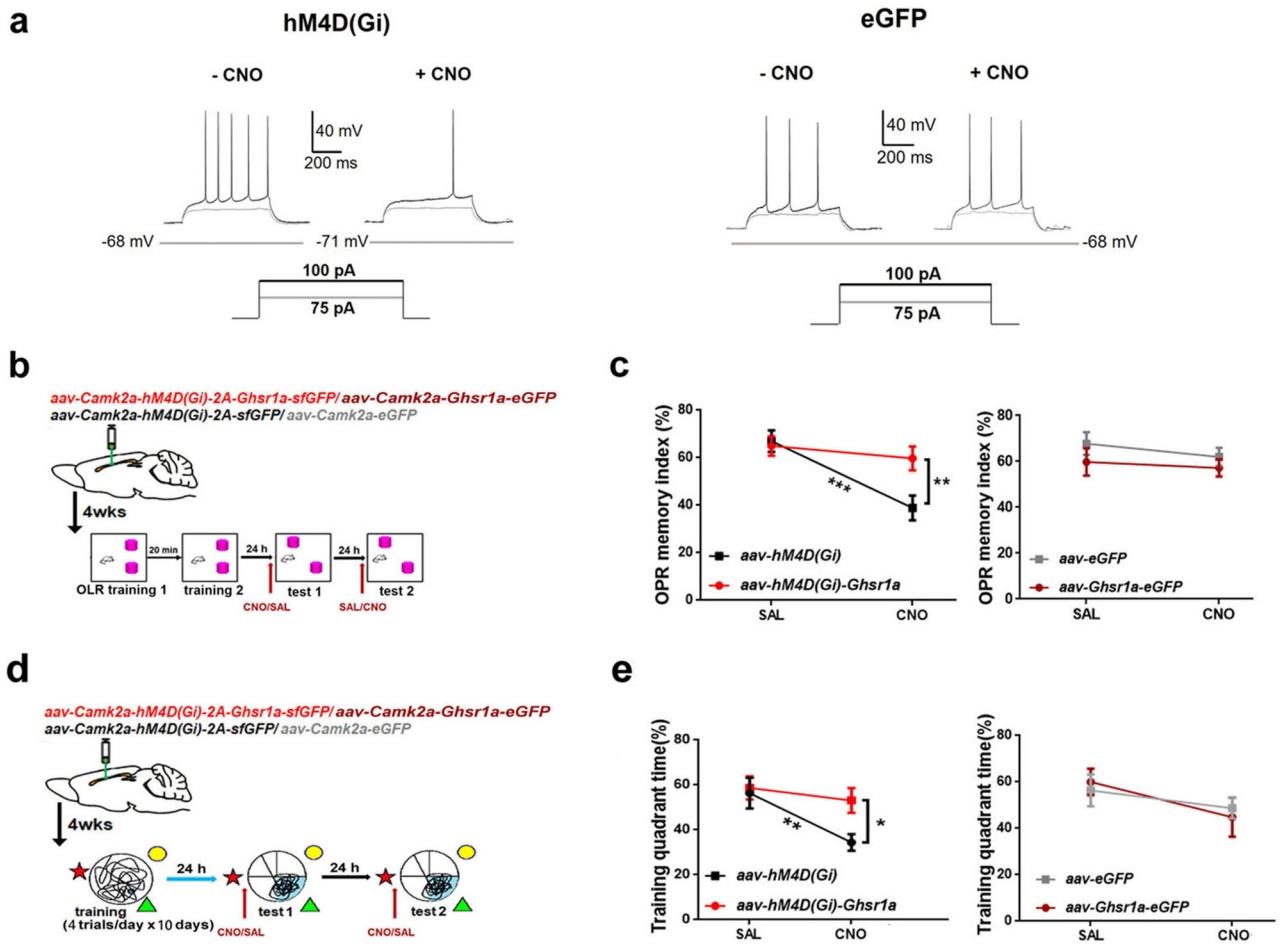

Fig. 5 | Chemogenetic inactivation of dCA1 pyramidal neurons with GHS-R1a overexpression impairs memory recall only in control mice. a Sample Ex vivo slice recordings. CNO, 20 μM. **b** Diagram illustrating experimental design. A strong OLR training protocol was adopted 4 weeks after virus injection in dCA1. CNO or SAL was applied by i.p. injection 45 min before the memory recall. **c** OLR memory assays for 4 groups of mice. ***Left***, CNO administration impaired OLR memory recall in control *aav-hM4D(Gi)* mice ($n = 10$), not in *aav-hM4D(Gi)-Ghsr1a* mice ($n = 11$). ***Right***, CNO injection does not affect memory recall in mice transduced with viruses without hM4Di construct ($n = 8$ mice per group). **d** Diagram illustrating experimental design. A strong MWM training protocol was applied 4 weeks after virus delivery. CNO or SAL was applied by i.p. injection 45 min before probe tests. **e** Spatial memory assays. ***Left***, CNO administration impaired spatial memory recall in control *aav-hM4D(Gi)* mice ($n = 6$), not in *aav-hM4D(Gi)-Ghsr1a* mice ($n = 8$). ***Right***, CNO injection does not affect memory recall in other two groups of mice ($n = 6$ mice per group). All data is shown as means ± SEM. $^{***}P < 0.001$, $^{**}P < 0.01$ or $^{*}P < 0.05$ means significant difference.

dCA1 area to selectively express both hM4Di and GHS-R1a, either hM4Di or GHS-R1a, or GFP only in pyramidal neurons. A strong OPR training protocol (2 trials with ITI of 20 min) or MWM training protocol (4 trials/2 blocks/day for 10 days) was adopted 4 weeks after virus injection to ensure that all groups of mice acquired good, comparable long-term memory. CNO (1 mg/kg) or normal saline (SAL) was i.p. injected 45 min before memory recall. Ex vivo slice recording confirmed that CNO (20 μM) administration selectively suppressed depolarization-evoked firing of pyramidal neurons expressing hM4Di, while had no effect on control neurons without hM4Di expression (Fig. 5a). As shown in Figs. 5b and 5c, after an intensive training, GHS-R1a-overexpressing mice exhibited similar OLR memory as controls (Fig. 5c Left; Two-way repeat-measure ANOVA, viral infection $F_{(1,\ 19)} = 18.31$, $P < 0.001$; drug treatment $F_{(1,\ 19)} = 3.04$, $P > 0.05$; interaction $F_{(1,\ 19)} = 8.62$, $P < 0.01$. Sidak's multiple comparisons test, *aav-hM4D(Gi)-Ghsr1a*/SAL mice vs. *aav-hM4D(Gi)*/SAL mice, $P > 0.05$. Figure 5c Right; *aav-Ghsr1a*/SAL mice vs. *aav-eGFP*/SAL mice, $P > 0.05$). Interestingly, we found that CNO administration impaired OLR memory recall only in control *aav-hM4D(Gi)* mice (Fig. 5c Left; *aav-hM4D(Gi)*/CNO vs. *aav-hM4D(Gi)*/SAL, $P < 0.001$), not in *aav-hM4D(Gi)-Ghsr1a* mice with high GHS-R1a expression (Fig. 5c Left; *aav-hM4D(Gi)-Ghsr1a*/CNO vs. *aav-hM4D(Gi)-Ghsr1a*/SAL, $P > 0.05$). GHS-R1a-overexpressing mice and controls exhibited different OLR memory recall only when receiving CNO injection (Fig. 5c Left; *aav-hM4D(Gi)-Ghsr1a*/CNO mice vs. *aav-hM4D(Gi)*/CNO mice, $P < 0.01$), not SAL injection. As expected, CNO injection did not affect memory recall in other two groups of mice transfected with viruses lacking the hM4Di construct (Fig. 5c Right; *aav-Ghsr1a*/CNO mice vs. *aav-eGFP*/CNO mice, $P > 0.05$). The finding that CNO treatment has no effect on memory recall of *aav-hM4D(Gi)-Ghsr1a* mice suggests that those dCA1 pyramidal neurons with high GHS-R1a expression may not be recruited to encode the OLR memory in the hippocampus.

Consistently, we found the same effect of CNO injection on the spatial memory recall (Fig. 5d, e). Specifically, CNO administration impaired spatial memory recall only in control *aav-hM4D(Gi)* mice (Fig. 5e Left; Two-way repeat-measure ANOVA, viral infection $F_{(1,\ 12)} = 18.28$, $P < 0.01$; drug treatment $F_{(1,\ 12)} = 3.05$, $P > 0.05$; interaction $F_{(1,\ 12)} = 4.596$, $P > 0.05$. Sidak's multiple comparisons test, *aav-hM4D(Gi)*/CNO vs. *aav-hM4D(Gi)*/SAL, $P < 0.01$), not in *aav-hM4D(Gi)-Ghsr1a* mice with high GHS-R1a expression (Fig. 5e Left; *aav-hM4D(Gi)-Ghsr1a*/CNO vs. *aav-hM4D(Gi)-Ghsr1a*/SAL, $P > 0.05$). Again, our findings demonstrated that, although GHS-R1a-

overexpressing mice obtained similar spatial memory as controls after an intensive MWM training (Fig. 5e Left; *aav-hM4D(Gi)-Ghsr1a* mice vs. *aav-hM4D(Gi)* mice, $P > 0.05$. Figure 5e Right; *aav-Ghsr1a* mice vs. *aav-eGFP* mice, $P > 0.05$), the dCA1 pyramidal neurons with high GHS-R1a expression may not participate in encoding a spatial memory in the hippocampus.

We used Tet-Off *aav-RAM-mKate2* viral system[20] to label the dCA1 neurons activated during memory retrieval, including engram cells. To this end, we first confirmed that feeding mice with Dox diet (on Dox) dramatically suppressed mKate2 expression, and following off Dox for 2 days was sufficient to permit robust mKate2-labeling of dCA1 neurons activated by spatial memory recall (Supplementary Fig. 4a-c). Also, we demonstrated that the majority of dCA1 neurons were labeled by mKate2 fluorescence following pentylenetetrazole (PTZ)-induced seizures with off Dox for 2 days (Supplementary Fig. 4d, e). We then injected Tet-Off *aav-RAM-mKate2* virus together with *aav-Camk2a-hM3D(Gq)-2A-Ghsr1a-sfGFP virus* or control *aav-Camk2a-hM3D(Gq)-2A-sfGFP* virus (mixture ratio 1:1) into mice dCA1 region. Dox diet was off 2 days before the probe test to permit labeling of dCA1 neurons that were activated during spatial memory retrieval (Fig. 6a, b). Our immunostaining analyses demonstrated that increasing GHS-R1a expression in pyramidal neurons dramatically reduced the total number of mKate2$^+$ cells (Fig. 6c, d; Two-way ANOVA, viral infection $F_{(1,\ 18)} = 79.35$, $P < 0.0001$; drug treatment $F_{(1,\ 18)} = 34.92$, $P < 0.0001$; interaction $F_{(1,\ 18)} = 2.10$, $P > 0.05$. Tukey's multiple comparisons test, *aav-hM3D(Gq)-Ghsr1a::RAM* /SAL group vs. control *aav-hM3D(Gq)::RAM* /SAL group, $P < 0.001$). CNO treatment during training increased the number of mKate2$^+$ cells in the dCA1 of GHS-R1a-overexpressing mice (Fig. 6d**;** *aav-hM3D(Gq)-Ghsr1a::RAM* /CNO group vs. *aav-hM3D(Gq)-Ghsr1a::RAM* /SAL group, $P < 0.05$). Notably, increasing GHS-R1a expression in dCA1 pyramidal neurons significantly reduced the portion of GFP$^+$mKate2$^+$ in total mKate2$^+$ cells (Fig. 6c, e; Two-way ANOVA, viral infection $F_{(1,\ 18)} = 66.44$, $P < 0.0001$; drug treatment $F_{(1,\ 18)} = 62.21$, $P < 0.0001$; interaction $F_{(1,\ 18)} = 0.47$, $P > 0.05$. Tukey's multiple comparisons test, *aav-hM3D(Gq)-Ghsr1a::RAM* /SAL group vs. *aav-hM3D(Gq)::RAM* /SAL group, $P < 0.0001$), and CNO administration during training antagonized such reduction caused by GHS-R1a overexpression (Fig. 6e; *aav-hM3D(Gq)-Ghsr1a::RAM* /CNO group vs. *aav-hM3D(Gq)-Ghsr1a::RAM* /SAL group, $P < 0.0001$). To further explore whether increasing GHS-R1a expression in dCA1 pyramidal neurons affects the engram size, we visualized neurons that were activated during the MWM training and reactivated during the probe test in combination of RAM system and c-Fos immunohistochemistry (Fig. 6f). Our results demonstrated that increasing GHS-R1a expression reduced both the number of mKate2$^+$ cells activated during memory encoding (Fig. 6g, h**;** Unpaired *t* test, $t = 4.52$, $P < 0.01$), and the number of mKate2$^+$c-Fos$^+$ engram cells that were activated during memory encoding and reactivated during memory recall (Fig. 6g, i**;** Unpaired *t* test, $t = 8.06$, $P < 0.001$), in dCA1 region of the hippocampus. These findings provide further evidence that high GHS-R1a expression in a relatively large population of dCA1 pyramidal neurons inhibits those neurons to participate in encoding spatial memory, and reduces engram size in the dCA1 region. Based on all these findings, we propose that an increase in GHS-R1a expression prevents targeted dCA1 pyramidal neurons from being recruited, resulting in reduced engram size in hippocampal dCA1 region, which is no longer sufficient to support a spatial memory. GHS-R1a-mediated suppression of neuronal excitability may play a key role in this process.

GHS-R1a deficiency rescues spatial memory deficit in APP/PS1 mice showing increased GHS-R1a expression

Previous studies reported increased GHS-R1a expression in the hippocampus of both AD patients and 5xFAD model mice[5]. We first confirmed increasing GHS-R1a expression in the whole hippocampus (Fig. 7a; Unpaired *t* test, APP/PS1 vs. WT mice, $t = 5.51$, $P < 0.001$), and the dCA1 region (Fig. 7b) of APP/PS1 mice. By use of the same Tet-Off RAM system, we compared the number of dCA1 neurons activated during the spatial memory recall among APP/PS1 mice, APP/PS1 mice with GHS-R1a deficiency (APP/PS1; GHS-R1a KO mice), and control WT mice (Fig. 7c). Our results demonstrated spatial memory deficit (Fig. 7d; One-way ANOVA, $F_{(2,\ 15)} = 5.20$, $P < 0.05$; Tukey's multiple comparisons test, target quadrant exploration: APP/PS1 vs. WT, $P < 0.05$), as well as reduced number of mKate2$^+$ neurons in the dCA1 of APP/PS1 mice (Fig. 7f, g; One-way ANOVA, $F_{(2,\ 15)} = 18.40$, $P < 0.0001$; Tukey's multiple comparisons test, APP/PS1 vs. WT, $P < 0.01$). Interestingly, we revealed that GHS-R1a deficiency rescued spatial memory deficit in APP/PS1 mice (Fig. 7d; APP/PS1; GHS-R1a KO mice vs. APP/PS1 mice, $P < 0.05$), meanwhile it restored the number of mKate2$^+$ neurons in the dCA1 of APP/PS1 mice (Fig. 7f, g; APP/PS1; GHS-R1a KO vs. APP/PS1 mice, $P < 0.0001$). Clearly, both WT mice and APP/PS1; GHS-R1a KO mice spent significantly more percentage of time than random (25%) navigating the training quadrant during the probe test (One sample *t* test, WT mice: $t = 3.63$, $P < 0.05$. APP/PS1; GHS-R1a KO mice: $t = 4.52$, $P < 0.05$), while the APP/PS1 mice did not (One sample *t* test, $t = 1.06$, $P > 0.05$). There were no group differences in swimming speed during the probe test (Fig. 7e; one-way ANOVA, $F_{(2,\ 15)} = 1.39$, $P > 0.05$). Hence, we concluded that the abnormal increase in GHS-R1a expression in the hippocampus contributes to impaired spatial memory encoding in APP/PS1 mice.

Discussion

GHS-R1a is a member of the class A G protein-coupled receptor (GPCR) that is widely distributed in the brain and in various immune cells[21]. It is the only receptor capable of interacting with acylated ghrelin to mediate neuronal functions of ghrelin/GHS-R1a signaling in the CNS, such as stimulating appetite in the hypothalamus and regulating memory processes in the hippocampus[3,22]. Besides ligand-dependent activity, the high constitutive/ligand-independent activity of GHS-R1a is speculated to contribute to the physiological importance of GHS-R1a signaling as well[8,9,23].

Although many studies have investigated the pharmacological effects of GHS-R1a activation on learning and memory by either systemic or local administration of ghrelin and GHS-R1a agonists, few studies have tested the importance of increasing GHS-R1a expression itself, regardless its elevation observed in the hippocampus of both AD patients and AD model mice[5]. In this study, we directly increased GHS-R1a expression in the hippocampus to test its effect on memory and associated engram as opposed to activating GHS-R1a by application of ghrelin or GHS-R1a agonists. One the other hand, we checked memory and the engram of APP/PS1 mice, a well-accepted AD model mice showing increased GHS-R1a expression in the hippocampus. Furthermore, we directly deleted GHS-R1a expression in APP/PS1 mice to examine its effect on memory and the engram. We found that virus-mediated GHS-R1a overexpression in dCA1 pyramidal neurons suppressed intrinsic excitability, blocked the recruitment of those neurons and hence reduced engram size in dCA1 region, leading to memory impairment. We also found that APP/PS1 mice exhibited increasing GHS-R1a expression in the hippocampus, reduced the number of dCA1 neurons activated during memory retrieval, and impaired spatial memory. Moreover, we demonstrated that GHS-R1a deletion restored the number of retrieval-activated neurons and rescued spatial memory deficit in APP/PS1 mice. In addition, our preliminary data shows that an increase in hippocampal GHS-R1a expression occurs as early as in 3-month-old APP/PS1 mice without significant memory impairments and Aβ pathologies. Altogether, our study thus provides several lines of evidence to support a causal and negative association between GHS-R1a expression in the hippocampus and memory. In addition, our findings, for the first time, reveal that GHS-R1a expression/activity regulates engram size, which may underlie its adverse effect on memory encoding.

In previous studies, we have demonstrated that ghrelin administration impairs multiple forms of learning and memory[15,16,24,25]. In particular, we reported recently that micro-infusion of ghrelin or non-peptide GHS-R1a agonist L-692,588 in dCA1 blocks the acquisition, not the consolidation of hippocampus-dependent memories by activating GHS-R1a and downstream PI3K/Akt signaling[16]. Present findings further strengthen our

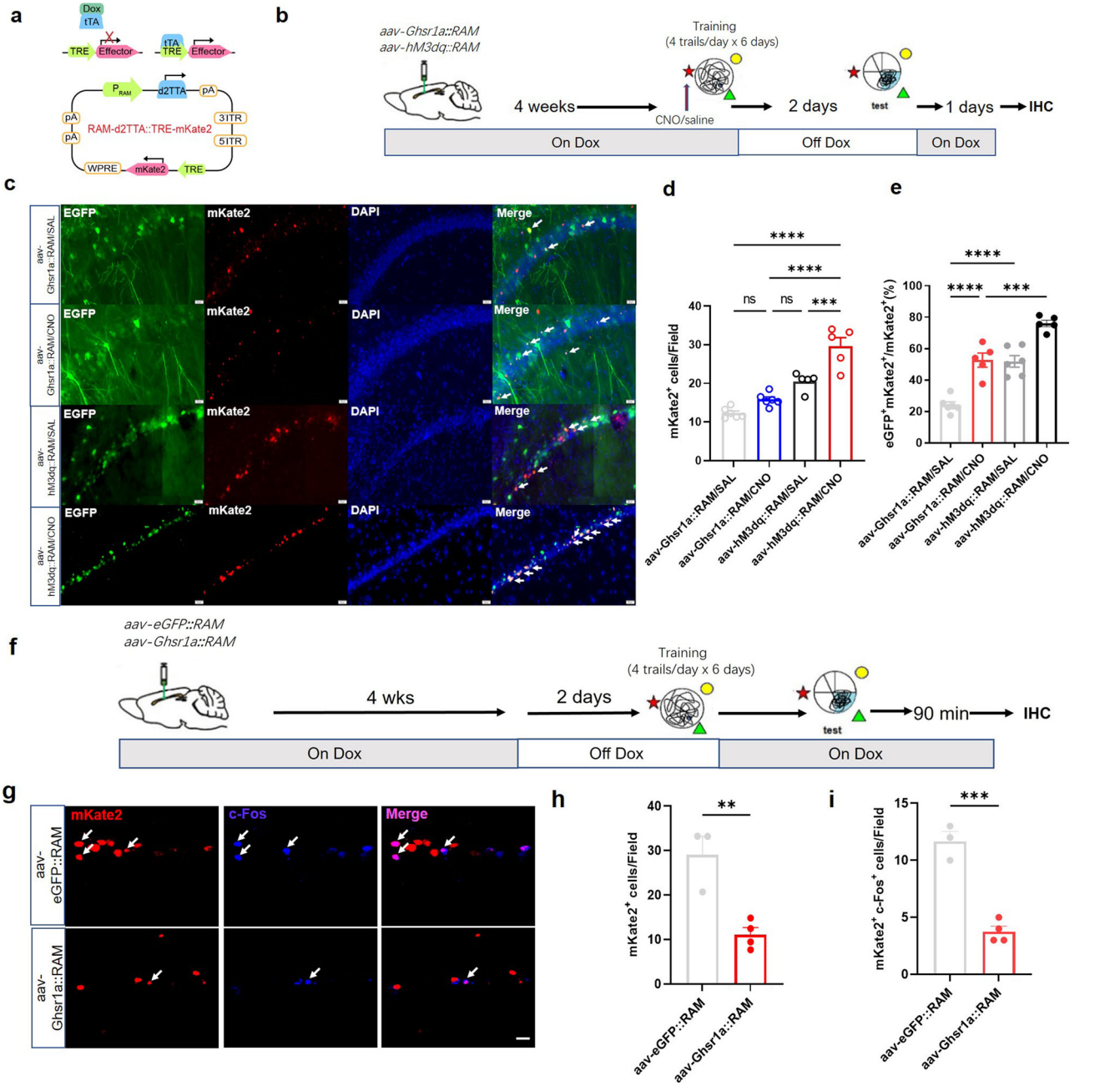

Fig. 6 | Increasing GHS-R1a expression impairs spatial memory allocation in dCA1 pyramidal neurons. a Schematic outline of the Tet-Off RAM viral system. Dox administration temporally shuts down the system. **b** A flow chart illustrating experiment design to label neurons activated during the spatial memory retrieval. Mice were bilaterally injected with a virus mixture of *aav-RAM-mKate2* and *aav-Camk2a-hM3D(Gq)-2A-hGhsr1a-eGFP*, or *aav-RAM-mKate2* and *aav-Camk2a-hM3D(Gq)-2A-eGFP* into the dCA1 region. Dox administration started 48 h before virus delivery, and withdrawn 48 h before the probe test, and resumed immediately after the probe test. CNO or SAL was administrated 30 min before training. **c** Representative images showing co-expression of mKate2 (red) and eGFP (green) in dCA1 pyramidal neurons of different groups of mice. Arrowheads indicate double positive neurons ($mKate2^+eGFP^+$). Scale bar, 20 μm. **d** The total number of $mKate2^+$ cells in dCA1 region. **e** The portion of $GFP^+mKate2^+$ cells in $mKate2^+$ cells in dCA1. 25 ~ 30 slices from 5–6 mice for each group. **f** A flow chart illustrating experiment design to label engram cells in dCA1 region. Mice were bilaterally injected with a virus mixture of *aav-RAM-mKate2* and *aav-Camk2a-Ghsr1a-GFP*, or *aav-RAM-mKate2* and *aav-Camk2a-eGFP* into the dorsal CA1. Dox was on 48 h before virus delivery, withdrawn 48 h before the MWM training, and resumed immediately after training. Immunostaining for c-Fos was done 90 min after the probe test. **g** Representative of images showing co-expression of mKate2(red) and c-Fos (blue) in dCA1 pyramidal neurons of different groups of mice. Arrowheads indicate positive neurons ($mKate2^+c\text{-}Fos^+$, Purple). Scale bar, 20 μm. **h** The total number of $mKate2^+$ cells in dCA1. **i** The total number of $mKate2^+c\text{-}Fos^+$ engram cells in dCA1. 15 ~ 20 slices from 3-4 mice for each group. All data are shown as means ± SEM. $^{****}P < 0.0001$, $^{***}P < 0.001$, $^{**}P < 0.001$, or $^{*}P < 0.05$ means significant difference.

statement that ghrelin/GHS-R1a signaling negatively regulates memory process by demonstrating that increasing GHS-R1a expression in dCA1 pyramidal neurons impairs memory encoding for both space and place. Our results apparently conflict with previous studies showing that ghrelin and ghrelin agonists facilitate learning and memory through activating GHS-R1a signaling in the hippocampus[3,26,27]. The reason for this discrepancy is unclear. It may result from different doses and duration of ghrelin treatment inducing distinct receptor kinetics. A previous study showed that transient and intensive GHS-R1a stimulation leads to rapid desensitization and internalization of the receptor that is slow to recover[28], while GHS-R1a

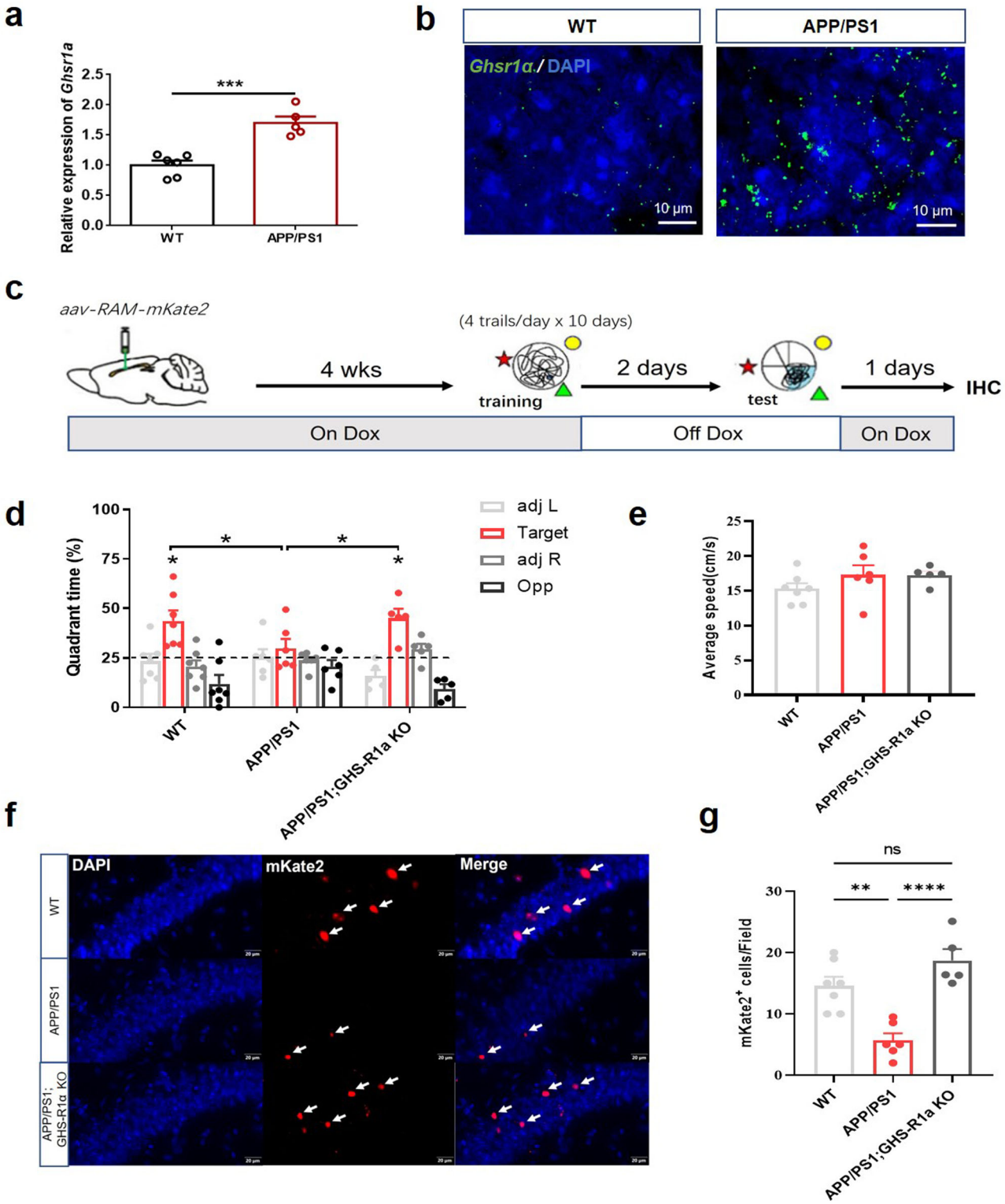

Fig. 7 | GHS-R1a deficiency rescues spatial memory deficit in APP/PS1 mice expressing increased GHS-R1a in the hippocampus. a RT-qPCR assays showing increased GHS-R1a expression in the hippocampus of APP/PS1 mice. n = 5–6 mice per group. **b** Representative of FISH imaging showing increased GHS-R1a expression in the dCA1 pyramidal cell layer. **c** A flow chart illustrating experiment design. *aav-RAM-mKate2* virus were bilaterally delivered into the dorsal CA1 region. Dox was on 48 h before virus delivery and withdrawn 48 h before the probe test, and resumed immediately after the probe test. **d** Quadrant searching time (%) during the MWM probe test. **e** Swimming speed during the MWM probe test. n = 5–7 mice per group. (**f**) Representative images showing memory recall-activated neurons (red) in dCA1 pyramidal cell layer. Scale bar, 20 μm. **g** Comparison of the total number of mKate2^{+} cells in dCA1 region. 25 ~ 35 slices from 5–7 mice for each group. All data are shown as means ± SEM. ***$P < 0.001$, **$P < 0.01$, or *$P < 0.05$ means significant difference.

internalization may habituate following either chronic administration of GHS-R1a agonist or chronic stress exposure[29]. Alternatively, different ghrelin treatment may trigger biased GHS-R1a signaling, such as G protein- or β-arrestin-dependent downstream pathways, leading to distinctive outcomes[30,31]. In previous studies[16], we locally applied a low dosage (8 ng) of ghrelin in the dCA1 and found similar results as selectively increasing GHS-R1a expression in dCA1 pyramidal neurons. Our findings are consistent with limited human data showing that serum ghrelin is inversely associated with cognitive function in both healthy individuals and patients with mild cognitive impairment (MCI)[32–34]. In addition, there are other animal studies showing that GHS-R1a knockout improved spatial memory[35]. Consistently, we recently reported that GHS-R1a global knockout mice displayed better hippocampus-dependent learning and memory than littermate controls[36].

Studies have highlighted the importance of ghrelin/GHS-R1a signaling in hippocampal synaptic physiology. For example, ghrelin has been reported to increase spine density and facilitate LTP induction in acute hippocampal slices[26], and to trigger synaptic incorporation of AMPA receptors in hippocampal cultures[27]. These findings provide possible synaptic mechanisms underlie ghrelin's promoting effect on memory consolidation or retention being reported previously[26,37–39]. In contrast, we found in previous studies that acute administration of ghrelin inhibited LTP in hippocampal SC-CA1 synapses, which may work together with reduced intrinsic excitability to contribute to ghrelin/GHS-R1a-induced impairment in memory acquisition[16]. In this study, we did not observe an effect of increased GHS-R1a expression on either synaptic transmission or plasticity at SC-CA1 excitatory synapses in acute hippocampal slices. The lack of synaptic modulation by virus-mediated GHS-R1a expression in dCA1 pyramidal neurons may be due to limited transfection efficiency or insufficient protein expression of the receptor in vivo. We thus presume that if increasing GHS-R1a expression in dCA1 pyramidal neurons does affect synaptic plasticity, it would be more likely to be an inhibition rather than a facilitation of excitatory synaptic activity. To support this notion, we did show, in a very recent study, that GHS-R1a knockout facilitates LTP at SC-CA1 excitatory synapses[36].

In addition to synaptic plasticity, the modulation of intrinsic excitability is considered another critical cellular mechanism underlying learning and memory[40–47].; In particular, conditioning induces a reduction of fAHP via downregulation of BK currents in hippocampal CA1 neurons, leading to increased excitability[40,44,45]. Memory recall induces a transient increase in the membrane resistance of DG engram cell by downregulation of Kir2.1 channels, resulting in high engram excitability that is associated with enhanced context recognition[47]. LTP, the prevalent cellular model for memory formation, induces an increase in dendritic excitability in CA1 cells, based on a hyperpolarized shift in the inactivation curve of A-type K^+ channels[42]. Conversely, hippocampal LTP induces a decrease in the excitability of CA1 neurons through the upregulation of I_h currents[43]. We have previously demonstrated that acute administration of ghrelin suppresses the intrinsic excitability of dCA1 pyramidal neurons by activating GHS-R1a and increasing fAHP amplitude[16]. Consistently, we found in the current study that selectively increasing GHS-R1a expression in dCA1 pyramidal neurons resulted in larger fAHP, longer ISI, wider AP half-width, and reduced firing rate, supporting reduced intrinsic excitability in these neurons. Additionally, we showed that chemogenetic activation of dCA1 pyramidal neurons with high GHS-R1a expression increases the firing rate while abolishing the upregulation of fAHP and AP half-width in these neurons. More importantly, we confirmed that memory impairment caused by GHS-R1a expression in dCA1 pyramidal neurons could be rescued either by blocking GHS-R1a activity during training with LEAP2, or by CNO-mediated activation of hM3Dq-DREADD resulting in an increase in the excitability of the same group of neurons. Therefore, based on the above-mentioned studies and our own findings, we propose that increasing GHS-R1a expression suppresses excitability by downregulating the BK currents, a key determinant of fAHP, in dCA1 pyramidal neurons, which may be a potential physiological mechanism underlying the negative impact of GHS-R1a on memory encoding. Since increasing GHS-R1a expression does not affect memory recall or LTP, it may have little effect on Kir2.1 channels[47], I_h currents[43], and A-type K^+ channels[42], the other key determinant of fAHP.

Unfortunately, our LEAP2 study cannot tell whether the effect of increasing GHS-R1a on memory formation depends on its constitutive activity, ligand binding, or both, given that LEAP2 acts as both an endogenous antagonist and inverse agonist of GHS-R1a, which may affect both ligand-dependent and ligand-independent activity of GHS-R1a[14]. Further studies using either ghrelin KO mice or GHS-R1a antagonists that selectively block ligand-dependent or constitutive activity are needed to answer this question. It also has to be mentioned that dCA1 pyramidal neurons show normal excitability in global GHS-R1a KO mice, perhaps due to compensation or circuit mechanisms that offsets the direct effect of GHS-R1a on excitability. GHS-R1a is reported to be highly localized in the hippocampus[48,49], with CA1 showing strong binding of biotinylated ghrelin[26] and the expression of GHS-R1a[50,51]. Previous studies have reported that GHS-R1a is mainly expressed in neurons[48,52]. Astrocytes also express GHS-R1a but not microglia[53]. Our FISH study demonstrated that GHS-R1a is expressed in both αCaMKII$^+$ pyramidal neurons and GAD65$^+$ interneurons in dCA1[36]. Based on these findings, we propose that suppressing the excitability of dCA1 pyramidal neurons is an important cellular mechanism mediating GHS-R1a-induced malfunction in hippocampal memory encoding.

Neuronal intrinsic excitability was reported to be involved in three different memory phases, including allocation, consolidation and updating[54]. Since ghrelin-dependent GHS-R1a activation disrupts acquisition, not the consolidation phase of memory processes[15,16], we hypothesized that increasing GHS-R1a expression and consequently decreasing excitability in a portion of dCA1 pyramidal neurons might affect cellular allocation of memories in the hippocampal network. Indeed, we found that hyperpolarizing high GHS-R1a neurons by CNO-mediated hM4Di-DREADD activation did not affect memory recall, suggesting that the ensembles of dCA1 pyramidal neurons with high level of GHS-R1a expression may no longer participate in memory encoding. Using a virus-based Tet-Off system to mark engram cells responsible for memory encoding, we further confirmed that increasing GHS-R1a expression reduced spatial engram size in dCA1region. Moreover, we demonstrated that increasing activity of high GHS-R1a neurons during the spatial training by CNO-mediated hM3Dq-DREADD promoted the participation of those neurons in memory encoding; meanwhile rescued memory impairment induced by GHS-R1a overexpression.

AD is the most common neurodegenerative disorder that is characterized by the accumulation of misfolded proteins resulting in irreversible memory decline and dementia over time[55]. Many studies have reported that ghrelin and GHS-R1a agonists improve AD-related pathogenesis, such as Aβ burden and Tau hyperphosphorylation in AD animal models, suggesting a therapeutic potential of ghrelin for AD treatment[56–58]. However, the mechanisms of ghrelin involvement in AD are unclear[59,60]. Given that plasma ghrelin is increased and negatively associated with cognitive deficits in AD patients[34,61], and GHSR-1a are significantly elevated in the hippocampi of both AD patients and AD mouse models[5], it is necessary to elucidate the effect and mechanism of ghrelin and GHS-R1a on AD pathology. Interestingly, here we discover that GHS-R1a deficiency restores the reduced number of dCA1 neurons activated during memory retrieval and rescues memory deficit in APP/PS1 mice showing increased GHS-R1a expression in the hippocampus. Engram is defined by cells activated at the time of memory encoding and reactivated at the time of memory retrieval. Studies have stated that the engram is essential to support a specific memory, and engram size is closely associated with memory performance[62,63]. Supportively, very recent studies demonstrate that the absence of a competitive neuronal engram allocation process in dCA1 of the immature hippocampus

precludes the formation of sparse engrams and precise memories[64]. However, too large or too small engram size may both cause memory impairment, given that the absolute number of neurons used to encode an episodic memory is relatively stable between nonhuman primates and rodents[65]. In particular, poor memory is associated with a reduced engram size in dCA1 region of the 9-month-old AD model mice[66]. Nevertheless, artificially increasing engram size causes fear memory deficits in mice[64]. Interestingly, other studies have reported no change of initial engram size in dCA1 of AD model mice[66–68]. In our study, we only labeled neurons activated during spatial memory retrieval, therefore, it is too early to tell whether spatial engram size in dCA1 is reduced in APP/PS1 mice due to increased GHS-R1a expression. Further experiments are needed to explore the causal relationship between GHS-R1a, engram size and AD-associated memory decline.

Current findings together with our previous studies[15,16,24,25] reveal that GHS-R1a negatively regulates memory under both physiological conditions and AD-associated pathological conditions. Consistently, a very recent study reported that neuronal ablation of GHS-R1a mitigates high-fat diet-induced memory impairment[69]. Although it is well reported that obesity is closely associated with cognitive dysfunction, including spatial memory deficits[70,71], it is unclear whether and how GHS-R1a contributes to obesity-related cognitive dysfunction. It should be interesting to test whether GHS-R1a expression in the hippocampus is increased in diet-induced obesity mice and how engram size changes accordingly. Furthermore, brain region-specific or cell type-specific regulation of GHS-R1a expression is much helpful to disclose the role and mechanism of GHS-R1a in both AD- and obesity-associated memory impairment.

In conclusion, our findings reveal, for the first time, a negative causal relationship between hippocampal GHS-R1a expression and memory encoding. Our findings suggest that reducing GHS-R1a expression or antagonizing GHS-R1a activity may be a promising approach to treat cognitive decline in pathophysiological conditions with GHS-R1a abnormality, such as AD.

Materials and methods

Mice

Male C57BL/6 J mice were purchased from the Vital River Laboratory Animal Technology Co. (Beijing, China). *Camk2a-Cre* mice (B6.Cg-Tg (Camk2a-cre) T29-1Stl/J, 005359) in C57BL/6 J background and APP/PS1 mice were from JAX. *Ghsr1a KO* mice in C57BL/6 J background were obtained from Shanghai Bio-Model Animals Research Center. APP/PS1;GHS-R1aKO mice(6-months old) were generated by intercrossing APP/PS1 mice and Ghsr1a KO mice. All genotypes were confirmed by PCR. Mice were group-housed at 20 ~ 22 °C on a 12 h:12 h light/dark cycle with free access to food and water. Only adult male mice at age of 12-20 weeks old were used for behavioral experiments. The Chancellor's Animal Research Committee at Qingdao University approved all animal protocols used in this study, in accordance with National Institutes of Health guidelines.

Virus injection in dCA1 region of the hippocampus

Mice were anaesthetized with 2.5% isoflurane and head-fixed on a stereotaxic frame. High titer AAV virus (10^13 GC/mL) were delivered bilaterally into dCA1 region through a glass needle connected to a WPI Nanoliter 2000 at a flow rate of 0.03 μl/min. GHS-R1a-overexpression virus (*aav-hSyn-DIO-Ghsr1a-eGFP, aav-Camk2a-Ghsr1a-eGFP, aav-Camk2a-hM3D(Gq)-2A-Ghsr1a*-sfGFP, *aav-Camk2a-hM4D(Gi)-2A-Ghsr1a*-sfGFP) and control virus (*aav-Camk2a-hM3D(Gq)-2A*-sfGFP, *aav-Camk2a-hM4D(Gi)-2A-sfGFP* and *aav-Camk2a-eGFP*) were prepared by Shanghai Obio Technology (China). The four injection coordinates were AP − 1.8 mm, ML ± 1 mm, DV − 1.5 mm and AP − 2.5 mm, ML ± 2 mm, DV − 1.6 mm relative to bregma. A volume of 0.15 μl virus was delivered to each injection site and the glass needle was left in the original position for an additional 10 min after injection to ensure optimal diffusion. Viral infection in dCA1 was confirmed by checking GFP fluorescence under an Olympus VS120 virtual slide microscope. Relative expression of *Ghsr1a* in the hippocampus was measured by qRT-PCR analysis. Experiments were performed 4 weeks after virus injection.

Local infusion of drugs in dCA1 region of the hippocampus

Stainless steel guide cannulas (OD 0.48 mm, ID 0.34 mm, RWD) were bilaterally implanted in the dCA1 according to the following coordinates: AP -2.0 mm, ML ± 1.5 mm and DV -1.0 mm relative to bregma. The cannulas were secured to the skull with stainless steel screws and dental cement. Mice were allowed to recover for 1 week before starting the experiment. Drugs were delivered in dCA1 through an injector cannula (OD 0.30 mm, ID 0.14 mm, RWD) pre-connected to a PE20 tubing (RWD) that was connected with a Hamilton syringe driven by a micro-infusion pump (Stoelting, USA) on the other end[8,24]. LEAP2 (4.3 μM, Phoenix Pharmaceuticals) were prepared in stock and freshly diluted with saline (SAL) to generate the final infusion solution. Drug dosage used for micro-infusion were chosen according to the literature and our previous studies[8,13,15]. The same volume of drug or saline vehicle (0.5 μl/side) were bilaterally delivered in dCA1 at 20 min before the experiment and with an interinfusion-interval of 20 min. The cannula was then left in position for an additional 5 min before withdrawal to prevent back-flow. Mice were kept conscious and were able to move freely during drug infusion.

Behavioral training and testing

All behavioral experiments were carried out during light cycle (9:00 am to 6:00 pm) in rooms with dim light. Mice were habituated in the experimental environment for at least 2 h before experiments. Animal behaviors were video-tracked and analyzed with Noldus EthoVision XT software except for fear memory assay.

Morris water maze (MWM). MWM is a typical behavior paradigm used to measure spatial learning and memory. A circular water pool (120 cm in diameter, 30 cm in depth) was divided evenly into four quadrants. During MWM training, an invisible escape platform (10 cm in diameter) was erected 0.5 cm underneath water surface. Mice were consecutively trained for 4 trials/2 blocks per day for 6 days, with an inter-block interval (IBI) of 1 h. A training trial ended whenever mice climbed onto the hidden platform or a cut-off time of 60 s, whichever was reached earlier. A probe test to evaluate spatial memory was carried out 1 h after same-day training at day 3 and day 5 respectively, and 24 h after the final day training. In probe tests, the hidden platform was removed and mice were allowed to navigate the pool for 60 s. The intensive training protocol consisted of 4 trials per day for 10 days.

Object-location recognition (OLR). OLR training and test were carried out in a non-transparent chamber (27.3 × 27.3 × 20.3 cm) with visual cures on the wall. During training, mice freely explored two identical objects inside the chamber for 10 min. The intensive training protocol consisted of two trials with an inter-trial interval (ITI) of 20 min. OLR memory was tested 24 h after training with one object transferred to a new location. Percentage of time mice exploring object in new location versus in old location was measured during a 5 min testing. Recognition Memory Index (%) was calculated as (exploration time for object in new location/total objects exploration time) x 100%.

Histology and immunostaining

Mice were anesthetized with isoflurane and transcardial perfusion was done first with 0.9% saline then with 4% paraformaldehyde (PFA). Whole brains were post-fixed in 4% PFA for additional 4 ~ 6 h, and then dehydrated in 30% sucrose for 48 h. Frozen brains were sectioned into 40 μm coronal slices with a Leica cryostat. The location of cannulas was checked with methylene blue staining. Only mice with proper cannula placement in the dCA1 were included in further analyses. Images were collected with virtual slide microscope (VS120, Olympus) with 10x or 20x objective lens.

Coronal slices were first blocked with 10% normal donkey serum (Jackson Immuno Research) for at least 1 h, and then incubated with

primary antibodies for overnight, and secondary antibodies for additional 1 h. Cells were counterstained with 4′,6-diamidino-2-Phenylindole (DAPI, 1:2000). Primary antibodies used were mouse anti-GFP (1:500, Millipore), rabbit anti-c-Fos (1:500, CST). Secondary antibodies were Alexa Fluor 488 goat anti-mouse IgG (1:1000, Invitrogen), Alexa Fluor 405 goat antirabbit IgG (1:1000, Invitrogen).

Fluorescence in situ hybridization (FISH)

Fluorescence in situ hybridization was performed with RNAscope Multiplex Fluorescent Reagent Kit V2 (ACD, 323100) following the manufacturer's instruction. Fresh brains were instantly frozen in isopentane, and coronal slices (14 μm in thickness) were mounted on SuperFrost Plus Gold slides (Fisher Scientific). After fixation in 4% PFA for 15 min at 4 ˚C, brain slices were dehydrated in 50%, 70%, and 100% ethanol in sequence, and finally air-dried at room temperature. RNA probes for *Camk2a*, *Gad1* and *Ghsr1a* mRNA were purchased from ACD. TSA Plus fluorescein, TSA Plus Cyanine 3 and TSA Plus Cyanine 5 were used to develop fluorescent signals visualized and captured by a Leica LAS-X confocal microscope with a 63x oil-immersion objective lens. Gain, threshold, and black levels remained unchanged during individual experiment.

Ex vivo slice electrophysiology

Fresh coronal slices were prepared with a Leica VT-1000 vibratome in an ice-cold cutting solution containing (in mM): 7 $MgSO_4$, 1 $CaCl_2$, 2.5 KCl, 26 $NaHCO_3$, 1 NaH_2PO_4, 30 Glucose, 1.3 sodium L-ascorbate, 1 kynurenic acid, 3 sodium pyruvate, and 119 choline chloride. Hippocampal slices (350 μm in thickness) were recovered in a submerged chamber containing a recovery solution containing (in mM): 85 NaCl, 2.5 KCl, 4 $MgCl_2$, 0.5 $CaCl_2$, 1.25 NaH_2PO_4, 24 $NaHCO_3$, 25 glucose, and 50 sucrose for at least 1 h at room temperature. Slices were then continuously perfused in a recording chamber with artificial cerebrospinal fluid (ACSF) at a rate of ~2 mL/min at 32 °C. All solutions (PH 7.2 ~ 7.4, Osmo 290 ~ 310) were oxygenated with 95% O_2 / 5% CO_2.

Whole-cell patch clamp recording in dCA1 pyramidal neurons was performed as previously described[47]. For current-clamp recording, glass electrodes (3 ~ 5 MΩ) were filled with an internal solution containing (in mM): 120 $KMeSO_4$, 10 KCl, 2 $MgCl_2$, 0.2 EGTA, 10 Hepes, 0.3 Na_3GTP, 4 Na_2ATP, 5 phosphocreatine. Step-current injections (600 ms or 50 ms in duration) were delivered from −50 pA in 25 pA increments. Resting membrane potential (RMP) was measured in current mode without current injection. The number of action potentials, input resistance, action potential threshold, AP half-width, inter-spike interval (ISI) between 1st and 2nd firings were measured in current mode with holding the cell at -70 mV and were analyzed with a custom Matlab program (R2018b). Only neurons that shows smaller RMP than −55 mV without spontaneous firing were used for analyses. Whole-cell voltage-clamp recordings were performed with electrodes filled with internal solution containing (in mM): 125 $CsCl_2$, 5 NaCl, 2 $MgCl_2$, 0.2 EGTA, 4 Hepes, 0.2 Na_3GTP, 2 MgATP, 7 phosphocreatine and 4 QX-314. Postsynaptic currents (PSCs) were detected at a holding potential of −60 mV, with 50 μM AP-5 and 50 μM picrotoxin in ACSF to isolate spontaneous excitatory postsynaptic currents (sEPSCs). Miniature excitatory postsynaptic currents (mEPSCs) were recorded separately with 1 μM TTX in ACSF. PSCs were analyzed by Mini Analysis Program.

Field excitatory postsynaptic potentials (fEPSPs) at the hippocampal Schaffer collateral-CA1 (SC-CA1) pathway were evoked every 30 s with a FHC bipolar platinum microelectrode[29,40]. The input-output (I/O) curve of basal synaptic transmission was constructed by varying stimulus intensity from 10 to 100 μA and measuring the pre-synaptic volley and the initial slope of corresponding fEPSPs. The paired-pulse ratio (PPR) was calculated by fEPSP2/fEPSP1 with variable inter-stimulus interval of 10, 25, 50, 100, 200, and 400 ms, respectively. Long-term potential (LTP) at SC-CA1 synapses was triggered by theta burst stimulation. All stimulating pulses were 100 μs in duration and 1/3–1/2 stimulation intensity that induces maximal fEPSP response. Recording was filtered at 2 kHz and digitized at 10 kHz. Data were acquired with MultiClamp 700B amplifier and pCLAMP 10.0 software (Molecular Devices). All chemicals used in electrophysiological recording were purchased from Sigma.

DREADDs and CNO injection

The chemogenetic technology DREADD (designer receptors exclusively activated by designer drugs), exclusively activated by the "designer drug" clozapine-N-oxide (CNO), is a powerful approach for transient manipulation of cellular activity both in vivo and ex vivo[72]. The hM4Di-DREADD is activated by CNO to inhibit neuronal activity and the hM3Dq-DREADD is activated by CNO to promote neuronal activity. CNO (Tocris) was initially dissolved in DMSO as 5 mg/ml stock solution, which was then diluted 500 times with normal saline (SAL) for in vivo experiment, and 1500 time with ACSF for ex vivo experiment. Animals received intraperitoneal (i.p.) injection of CNO (1 mg/kg) or same amount of saline 45 min before behavioral training or test. Slice physiology was done 10-15 min after CNO perfusion[36].

Quantitative reverse transcription PCR (RT-qPCR)

Total RNA was extracted from the hippocampus with the PureLink™ RNA Mini Kit (Thermo Fisher Scientific). RNA quantity and quality were measured using a NanoDrop 2000 Spectrophotometer (Thermo Fisher Scientific). Complementary DNA was synthesized from 1 μg of total RNA with SuperScript™ III Reverse Transcriptase (Invitrogen). PCR-based quantification of *Ghsr1a* was performed using a MasterCycler® ep realplex PCR system (Eppendorf) and a QuantiFast SYBR Green PCR Kit (Qiagen). The PCR cycling parameters were as follows: 95 °C for 5 min, followed by 40 cycles of PCR reaction at 95 °C for 5 s, 60 °C for 30 s, 72 °C for 30 s. $2^{-\Delta\Delta CT}$ method was used to normalize CT values against housekeeping gene *Actb* and quantify relative expression of *Ghsr1a* in the *Ghsr1a* KO mice and *Ghsr1a* overexpression mice. PCR primer sequences (Thermo Fisher Scientific) used were as follows: *Ghsr-F GTATGGGTGTCGAGCGTCTT, Ghsr-R AGCCAGCAGAGGATGAAAGC; Actb-F CATCCGTAAAGACCTCTATGCCAAC, Actb-R ATGGAGCCACCGATCCACA*. Triplicates were done for each sample.

Activity-dependent cell labeling

P-RAM-based Tet-Off system was used to label activity-dependent cells in the hippocampus[20]. Mice were bilaterally injected with a virus mixture (150 nL of *aav-RAM-mKate2* and 150 nL of the *aav-Camk2a-hM3D(Gq)-2A-hGhsr1a-GFP*) or a virus mixture (150 nL of *aav-RAM-mKate2* and 150 nL *aav-Camk2a-hM3D(Gq)-2A-EGFP*) into the dorsal CA1. Mice were fed with chow containing doxycycline (Dox, 40 mg/kg) to shut down the system shortly after virus delivery. Either saline or CNO (1 mg g/kg, i.p.) was administrated (i.p.) 30 min before MWM training. Dox was then withdrawn 48 h before the MWM training or the probe test to open a permissive time window for tagging of neurons activated during spatial memory acquisition or retrieval. Dox treatment wasthen resumed immediately after the training or the probe test. Perfusion and brains fixation were done 24 h later. Frozen brains were sectioned into 40 μm coronal slices with a Leica cryostat. Immunostaining images were captured on a laser confocal microscope (LAS-X; Leica) and analyzed using Image J software. For quantitative analyses, 5 ~ 6 coronal hippocampal sections/mouse were counted and averaged, with 5 ~ 6 mice/group. The numbers of $mKate2^+$ cells, $mKate2^+c\text{-}Fos^+$ cells, and the ratios of $mKate2^+GFP^+$cells/ $mKate2^+$ cells in dCA1 were counted and calculated.

Drug-induced seizures

Pharmacologically induced seizures were used to drive maximal RAM expression in the hippocampus. Mice were given intraperitoneal injections of 50 mg/kg pentylenetetrazole (PTZ, Sigma), and were selected for further analysis only if they exhibited full motor seizures.

Statistics and reproducibility

Results were expressed as means ± SEM. Data were analyzed using one-sample *t* test, unpaired *t* test, one-way ANOVA, or two-way ANOVA with appropriate multiple comparisons test, as indicated in the content. $P < 0.05$

indicates significant difference between groups. Statistical analysis was performed with GraphPad Prism 6.0 (GraphPad Software).

Reporting summary

Further information on research design is available in the Nature Portfolio Reporting Summary linked to this article.

Data availability

The data that support the findings of this study are available in the Supplementary Data file. All other data are available from the corresponding author on reasonable request. Source data underlying the graphs in the main and Supplementary Figs. are provided as supplementary data.

Received: 21 March 2024; Accepted: 17 September 2024;
Published online: 16 October 2024

References

1. Kojima, M. et al. Ghrelin is a growth-hormone-releasing acylated peptide from stomach. *Nature* **402**, 656–660 (1999).
2. Perello, M. et al. Brain accessibility delineates the central effects of circulating ghrelin. *J. Neuroendocrinol.* **31**, e12677 (2019).
3. Andrews, Z. B. The extra-hypothalamic actions of ghrelin on neuronal function. *Trends Neurosci.* **34**, 31–40 (2011).
4. Spencer, S. J., Emmerzaal, T. L., Kozicz, T. & Andrews, Z. B. Ghrelin's Role in the Hypothalamic-Pituitary-Adrenal Axis Stress Response: Implications for Mood Disorders. *Biol. Psychiatry* **78**, 19–27 (2015).
5. Tian, J. et al. Disrupted hippocampal growth hormone secretagogue receptor 1α interaction with dopamine receptor D1 plays a role in Alzheimer's disease. *Sci. Transl. Med.* **11** (2019).
6. Holst, B., Cygankiewicz, A., Jensen, T. H., Ankersen, M. & Schwartz, T. W. High constitutive signaling of the ghrelin receptor–identification of a potent inverse agonist. *Mol. Endocrinol.* **17**, 2201–2210 (2003).
7. Petersen, P. S. et al. In vivo characterization of high Basal signaling from the ghrelin receptor. *Endocrinology* **150**, 4920–4930 (2009).
8. Li, N. et al. Blocking constitutive activity of GHSR1a in the lateral amygdala facilitates acquisition of conditioned taste aversion. *Neuropeptides* **68**, 22–27 (2018).
9. Torz, L. J. et al. Metabolic insights from a GHSR-A203E mutant mouse model. *Mol. Metab.* **39**, 101004 (2020).
10. Schellekens, H., van Oeffelen, W. E., Dinan, T. G. & Cryan, J. F. Promiscuous dimerization of the growth hormone secretagogue receptor (GHS-R1a) attenuates ghrelin-mediated signaling. *J. Biol. Chem.* **288**, 181–191 (2013).
11. Kern, A. et al. Hippocampal Dopamine/DRD1 Signaling Dependent on the Ghrelin Receptor. *Cell* **163**, 1176–1190 (2015).
12. Wallace Fitzsimons, S. E. et al. A ghrelin receptor and oxytocin receptor heterocomplex impairs oxytocin mediated signalling. *Neuropharmacology* **152**, 90–101 (2019).
13. Ge, X. et al. LEAP2 Is an Endogenous Antagonist of the Ghrelin Receptor. *Cell Metab.* **27**, 461–469 e466 (2018).
14. Mani, B. K. et al. LEAP2 changes with body mass and food intake in humans and mice. *J. Clin. Invest* **129**, 3909–3923 (2019).
15. Song, L. et al. Ghrelin modulates lateral amygdala neuronal firing and blocks acquisition for conditioned taste aversion. *PLoS One* **8**, e65422 (2013).
16. Li, N. et al. Ghrelin signaling in dCA1 suppresses neuronal excitability and impairs memory acquisition via PI3K/Akt/GSK-3β cascades. *Neuropharmacology* **203**, 108871 (2022).
17. Zhou, Y. et al. CREB regulates excitability and the allocation of memory to subsets of neurons in the amygdala. *Nat. Neurosci.* **12**, 1438–1443 (2009).
18. Yiu, A. P. et al. Neurons are recruited to a memory trace based on relative neuronal excitability immediately before training. *Neuron* **83**, 722–735 (2014).
19. Mocle, A. J. et al. Excitability mediates allocation of pre-configured ensembles to a hippocampal engram supporting contextual conditioned threat in mice. *Neuron* **112**, 1487–1497 e1486 (2024).
20. Sørensen, A. T. et al. A robust activity marking system for exploring active neuronal ensembles. *Elife* **5**, 13918 (2016).
21. Guan, X. M. et al. Distribution of mRNA encoding the growth hormone secretagogue receptor in brain and peripheral tissues. *Brain Res Mol. Brain Res* **48**, 23–29 (1997).
22. Yanagi, S., Sato, T., Kangawa, K. & Nakazato, M. The Homeostatic Force of Ghrelin. *Cell Metab.* **27**, 786–804 (2018).
23. Fernandez, G. et al. Evidence Supporting a Role for Constitutive Ghrelin Receptor Signaling in Fasting-Induced Hyperphagia in Male Mice. *Endocrinology* **159**, 1021–1034 (2018).
24. Zhu, Q. et al. Ghrelin but not nesfatin-1 affects certain forms of learning and memory in both rats and mice. *Brain Res* **1541**, 42–51 (2013).
25. Zhao, Z. et al. Ghrelin administration enhances neurogenesis but impairs spatial learning and memory in adult mice. *Neuroscience* **257**, 175–185 (2014).
26. Diano, S. et al. Ghrelin controls hippocampal spine synapse density and memory performance. *Nat. Neurosci.* **9**, 381–388 (2006).
27. Ribeiro, L. F. et al. Ghrelin triggers the synaptic incorporation of AMPA receptors in the hippocampus. *Proc. Natl Acad. Sci. USA* **111**, E149–E158 (2014).
28. Camiña, J. P. et al. Desensitization and endocytosis mechanisms of ghrelin-activated growth hormone secretagogue receptor 1a. *Endocrinology* **145**, 930–940 (2004).
29. Meyer, R. M., Burgos-Robles, A., Liu, E., Correia, S. S. & Goosens, K. A. A ghrelin-growth hormone axis drives stress-induced vulnerability to enhanced fear. *Mol. Psychiatry* **19**, 1284–1294 (2014).
30. Gross, J. D. et al. Discovery of a functionally selective ghrelin receptor (GHSR(1a)) ligand for modulating brain dopamine. *Proc. Natl Acad. Sci. USA* **119**, e2112397119 (2022).
31. Rouault, A. A. J. et al. The GPCR accessory protein MRAP2 regulates both biased signaling and constitutive activity of the ghrelin receptor GHSR1a. *Sci. Signal.* **13** (2020).
32. Spitznagel, M. B. et al. Serum ghrelin is inversely associated with cognitive function in a sample of non-demented elderly. *Psychiatry Clin. Neurosci.* **64**, 608–611 (2010).
33. Yoshino, Y. et al. Ghrelin cascade changes in the peripheral blood of Japanese patients with Alzheimer's disease. *J. Psychiatr. Res* **107**, 79–85 (2018).
34. Cao, X. et al. Increased Serum Acylated Ghrelin Levels in Patients with Mild Cognitive Impairment. *J. Alzheimers Dis.* **61**, 545–552 (2018).
35. Albarran-Zeckler, R. G., Brantley, A. F. & Smith, R. G. Growth hormone secretagogue receptor (GHS-R1a) knockout mice exhibit improved spatial memory and deficits in contextual memory. *Behav. Brain Res* **232**, 13–19 (2012).
36. Li, N. et al. GHSR1a deficiency suppresses inhibitory drive on dCA1 pyramidal neurons and contributes to memory reinforcement. *Cereb. Cortex* **33**, 2612–2625 (2023).
37. Carlini, V. P. et al. Ghrelin increases anxiety-like behavior and memory retention in rats. *Biochem Biophys. Res Commun.* **299**, 739–743 (2002).
38. Chen, L. et al. Local infusion of ghrelin enhanced hippocampal synaptic plasticity and spatial memory through activation of phosphoinositide 3-kinase in the dentate gyrus of adult rats. *Eur. J. Neurosci.* **33**, 266–275 (2011).
39. Ghersi, M. S. et al. Ghrelin increases memory consolidation through hippocampal mechanisms dependent on glutamate release and NR2B-subunits of the NMDA receptor. *Psychopharmacol. (Berl.)* **232**, 1843–1857 (2015).
40. Disterhoft, J. F., Coulter, D. A. & Alkon, D. L. Conditioning-specific membrane changes of rabbit hippocampal neurons measured in vitro. *Proc. Natl Acad. Sci. USA* **83**, 2733–2737 (1986).

41. Zhang, W. & Linden, D. J. The other side of the engram: experience-driven changes in neuronal intrinsic excitability. *Nat. Rev. Neurosci.* **4**, 885–900 (2003).
42. Frick, A., Magee, J. & Johnston, D. LTP is accompanied by an enhanced local excitability of pyramidal neuron dendrites. *Nat. Neurosci.* **7**, 126–135 (2004).
43. Fan, Y. et al. Activity-dependent decrease of excitability in rat hippocampal neurons through increases in I(h). *Nat. Neurosci.* **8**, 1542–1551 (2005).
44. Matthews, E. A., Weible, A. P., Shah, S. & Disterhoft, J. F. The BK-mediated fAHP is modulated by learning a hippocampus-dependent task. *Proc. Natl Acad. Sci. USA* **105**, 15154–15159 (2008).
45. Matthews, E. A., Linardakis, J. M. & Disterhoft, J. F. The fast and slow afterhyperpolarizations are differentially modulated in hippocampal neurons by aging and learning. *J. Neurosci.* **29**, 4750–4755 (2009).
46. Oh, M. M. & Disterhoft, J. F. Increased Excitability of Both Principal Neurons and Interneurons during Associative Learning. *Neuroscientist* **21**, 372–384 (2015).
47. Pignatelli, M. et al. Engram Cell Excitability State Determines the Efficacy of Memory Retrieval. *Neuron* **101**, 274–284 e275 (2019).
48. Zigman, J. M., Jones, J. E., Lee, C. E., Saper, C. B. & Elmquist, J. K. Expression of ghrelin receptor mRNA in the rat and the mouse brain. *J. Comp. Neurol.* **494**, 528–548 (2006).
49. Mani, B. K. et al. Neuroanatomical characterization of a growth hormone secretagogue receptor-green fluorescent protein reporter mouse. *J. Comp. Neurol.* **522**, 3644–3666 (2014).
50. Jiang, H., Betancourt, L. & Smith, R. G. Ghrelin amplifies dopamine signaling by cross talk involving formation of growth hormone secretagogue receptor/dopamine receptor subtype 1 heterodimers. *Mol. Endocrinol.* **20**, 1772–1785 (2006).
51. Xu, L. et al. The stimulating effect of ghrelin on gastric motility and firing activity of gastric-distension-sensitive hippocampal neurons and its underlying regulation by the hypothalamus. *Exp. Physiol.* **99**, 123–135 (2014).
52. Muniz, B. G. & Isokawa, M. Ghrelin receptor activity amplifies hippocampal N-methyl-d-aspartate receptor-mediated postsynaptic currents and increases phosphorylation of the GluN1 subunit at Ser896 and Ser897. *Eur. J. Neurosci.* **42**, 3045–3053 (2015).
53. Fuente-Martín, E. et al. Ghrelin Regulates Glucose and Glutamate Transporters in Hypothalamic Astrocytes. *Sci. Rep.* **6**, 23673 (2016).
54. Chen, L. et al. The role of intrinsic excitability in the evolution of memory: Significance in memory allocation, consolidation, and updating. *Neurobiol. Learn Mem.* **173**, 107266 (2020).
55. Selkoe, D. J. Alzheimer's disease: genes, proteins, and therapy. *Physiol. Rev.* **81**, 741–766 (2001).
56. Moon, M., Cha, M. Y. & Mook-Jung, I. Impaired hippocampal neurogenesis and its enhancement with ghrelin in 5XFAD mice. *J. Alzheimers Dis.* **41**, 233–241 (2014).
57. Eslami, M., Sadeghi, B. & Goshadrou, F. Chronic ghrelin administration restores hippocampal long-term potentiation and ameliorates memory impairment in rat model of Alzheimer's disease. *Hippocampus* **28**, 724–734 (2018).
58. Jeong, Y. O. et al. MK-0677, a Ghrelin Agonist, Alleviates Amyloid Beta-Related Pathology in 5XFAD Mice, an Animal Model of Alzheimer's Disease. *Int. J. Mol. Sci.* **19** (2018).
59. Jeon, S. G. et al. Ghrelin in Alzheimer's disease: Pathologic roles and therapeutic implications. *Ageing Res Rev.* **55**, 100945 (2019).
60. Reich, N. & Hölscher, C. Acylated Ghrelin as a Multi-Targeted Therapy for Alzheimer's and Parkinson's Disease. *Front Neurosci.* **14**, 614828 (2020).
61. Shibata, N., Ohnuma, T., Kuerban, B., Komatsu, M. & Arai, H. Genetic association between ghrelin polymorphisms and Alzheimer's disease in a Japanese population. *Dement Geriatr. Cogn. Disord.* **32**, 178–181 (2011).
62. Leake, J., Zinn, R., Corbit, L. H., Fanselow, M. S. & Vissel, B. Engram Size Varies with Learning and Reflects Memory Content and Precision. *J. Neurosci.* **41**, 4120–4130 (2021).
63. Guskjolen, A. & Cembrowski, M. S. Engram neurons: Encoding, consolidation, retrieval, and forgetting of memory. *Mol. Psychiatry* **28**, 3207–3219 (2023).
64. Stefanelli, T., Bertollini, C., Lüscher, C., Muller, D. & Mendez, P. Hippocampal Somatostatin Interneurons Control the Size of Neuronal Memory Ensembles. *Neuron* **89**, 1074–1085 (2016).
65. Thome, A. et al. Evidence for an Evolutionarily Conserved Memory Coding Scheme in the Mammalian Hippocampus. *J. Neurosci.* **37**, 2795–2801 (2017).
66. Roy, D. S. et al. Memory retrieval by activating engram cells in mouse models of early Alzheimer's disease. *Nature* **531**, 508–512 (2016).
67. Perusini, J. N. et al. Optogenetic stimulation of dentate gyrus engrams restores memory in Alzheimer's disease mice. *Hippocampus* **27**, 1110–1122 (2017).
68. Poll, S. et al. Memory trace interference impairs recall in a mouse model of Alzheimer's disease. *Nat. Neurosci.* **23**, 952–958 (2020).
69. Wang, H. et al. Neuronal ablation of GHSR mitigates diet-induced depression and memory impairment via AMPK-autophagy signaling-mediated inflammation. *Front Immunol.* **15**, 1339937 (2024).
70. André, C., Dinel, A. L., Ferreira, G., Layé, S. & Castanon, N. Diet-induced obesity progressively alters cognition, anxiety-like behavior and lipopolysaccharide-induced depressive-like behavior: focus on brain indoleamine 2,3-dioxygenase activation. *Brain Behav. Immun.* **41**, 10–21 (2014).
71. Wang, H. Y. et al. Huperzine A ameliorates obesity-related cognitive performance impairments involving neuronal insulin signaling pathway in mice. *Acta Pharm. Sin.* **41**, 145–153 (2020).
72. Gomez, J. L. et al. Chemogenetics revealed: DREADD occupancy and activation via converted clozapine. *Science* **357**, 503–507 (2017).

Acknowledgements

This work was supported by NSFC (Grant no. 32071141 and 32371211 to YZ), NSF of SD province (no. ZR2019ZD34 to YZ, no. ZR201911120651 to NL, and no. ZR2023MH051 to MY), and NSF of Qingdao (no. 23-2-1-188-zyyd-jch to MY). We thank Mr. Vincent Li for native language editing.

Author contributions

Y.Z., N.L. and H.Y. designed and supervised the experiments. M.Z., L.Y., J.J., F.X., S.G. and M.D. performed behavioral experiments, N.L. and L.Y. performed electrophysiological experiments, M.Z., J.J., F.X. and S.G. performed virus injection, J.J., F.H., M.Y. and J.W. performed biochemical analyses. J.W., V.L. and M.Y. helped with data analysis. Y.S., L.Y. and Y.Z. wrote the manuscript. All authors read and approved the final manuscript.

Competing interests

The authors declare no competing interests.

Additional information

Supplementary information The online version contains supplementary material available at https://doi.org/10.1038/s42003-024-06914-y.

Correspondence and requests for materials should be addressed to Yu Zhou or Nan Li.

Peer review information *Communications Biology* thanks the anonymous reviewers for their contribution to the peer review of this work. Primary Handling Editor: Benjamin Bessieres. A peer review file is available.